



RESEARCH ARTICLE

Spatio-temporal evaluation of gridded precipitation products for the high-altitude Indus basin

Zakir Hussain Dahri^{1,2}  | Fulco Ludwig¹ | Eddy Moors^{3,4} | Shakil Ahmad⁵ | Bashir Ahmad² | Muhammad Shoaib⁶ | Irfan Ali² | Muhammad Shahid Iqbal⁷ | Muhammad Saleem Pomee^{2,8}  | Abdul Ghafoor Mangrio² | Muhammad Munir Ahmad² | Pavel Kabat^{1,9}

¹Water Systems and Global Change, Wageningen University and Research, Wageningen, The Netherlands

²Natural Resources Division, Pakistan Agricultural Research Council, Islamabad, Pakistan

³IHE Delft Institute for Water Education, Delft, The Netherlands

⁴Earth and Climate Cluster, Faculty of Earth and Life Sciences, VU University Amsterdam, Amsterdam, The Netherlands

⁵NUST Institute of Civil Engineering, National University of Sciences and Technology, Islamabad, Pakistan

⁶Department of Agricultural Engineering, Bahauddin Zakariya University, Multan, Pakistan

⁷Department of Space Science, Institute of Space Technology, Islamabad, Pakistan

⁸Institute of Geography, Chair of Regional Climate and Hydrology, University of Augsburg, Augsburg, Germany

⁹World Meteorological Organization, Geneva, Switzerland

Correspondence

Zakir Hussain Dahri, Water Systems and Global Change, Wageningen University and Research, Wageningen, The Netherlands.

Email: zakir.dahri@wur.nl and zakirdahri@yahoo.com

Funding information

Netherlands Organization for International Cooperation in Higher Education through Netherlands Fellowship Program, Grant/Award Number: NFP-PhD.11/ 898

Abstract

The high-altitude Indus basin is one of the most complex and inadequately explored mountain terrains in the World, where reliable observations of precipitation are highly lacking. Therefore, spatially distributed precipitation products developed at global/regional scale are often used in several scientific disciplines. However, large uncertainties in precipitation estimates of such precipitation data sets often lead to suboptimal outcomes. In this study, performance of 27 widely used gridded precipitation products belonging to three different categories of gauge-based, reanalysis and merged products is evaluated with respect to high-quality reference climatologies of mean monthly precipitation. Widely used statistical measures and quantitative analysis techniques are used to analyse the spatial patterns and quantitative distribution of mean monthly, seasonal and annual precipitation at sub-regional scale. Mean annual precipitation estimates of the gridded data sets are cross validated with the corresponding adjusted streamflows using Turc-Budyko non-dimensional analysis. Results reveal poor to moderately good performance of the gridded data sets. Marked differences in spatiotemporal and quantitative distribution of precipitation are found among the data sets. All data sets are consistent in their patterns showing negative or dry bias in wet areas and

This is an open access article under the terms of the Creative Commons Attribution License, which permits use, distribution and reproduction in any medium, provided the original work is properly cited.

© 2021 The Authors. *International Journal of Climatology* published by John Wiley & Sons Ltd on behalf of Royal Meteorological Society.

positive or wet bias in dry areas, although considerable differences in the magnitudes of the biases are noticed at sub-regional scale. None of the data sets is equally good for all sub-regions due to very high spatiotemporal variability in their performance at sub-regional scale. Gauge-based and merged products performed better in dry regions and during monsoon season, while reanalysis products provided better estimates in wet areas and during winter months. GPCC V8, ERA5 and MSWEP2.2 are found better than their counter-grouped data sets. Overall, ERA5 is found most acceptable for all sub-regions, particularly at higher-altitudes, in wet areas and during winter months.

KEYWORDS

evaluation, Indus basin, precipitation distribution, precipitation products, precipitation uncertainties

1 | INTRODUCTION

Precipitation is the principal source of freshwater supplies that plays a crucial role in socioeconomic developments, environmental integrity and sustaining life on earth. Naturally, precipitation is discontinuous in space and time, has intricate characteristics, can occur in several forms, and its causal mechanisms can influence precipitation from cloud to cyclone scales. Errors in precipitation data can have significant implications for climate and water balance studies. It is therefore essential to accurately measure/estimate precipitation at higher spatiotemporal resolutions. This is particularly important in orographically influenced high-mountain terrains where precipitation often changes abruptly over short distances (Anders *et al.*, 2006) and majority of it falls as snow. A high-quality, dense and adequately representative network of observations is essential to precisely measure occurrence, quantity and type of precipitation.

The high-altitude Indus basin is one of the most complex and largely underexplored regions in the World. Its climate and precipitation are largely modulated by a couple of synoptic-scale atmospheric circulation systems: the Indian summer monsoon and the winter westerlies (Wang and Lin, 2002; Ding and Chan, 2005; Yao *et al.*, 2012; Pang *et al.*, 2014). The Indian summer monsoon advects moisture through several trajectories originating from the Bay of Bengal, Indian Ocean and Arabian Sea due to the differential heating between land and sea (Böhner, 2006; Hodges, 2006; Bolch *et al.*, 2012; Yao *et al.*, 2012; Pang *et al.*, 2014). It causes heavy rainfall in south-eastern areas during June–September and moves north-westward along the Himalayan Arc with decreasing strength. The winter westerlies transport large masses of moist air from the Caspian, Black and Mediterranean seas and North Atlantic Ocean throughout the year and

are the dominant source of precipitation in the Hindukush, Karakoram and to a lesser extent in the W-Himalayan regions during December–April months (Böhner, 2006; Syed *et al.*, 2006; Treydte *et al.*, 2006; Filippi *et al.*, 2014; Mayer *et al.*, 2014; Pal *et al.*, 2014). Moreover, significant amount of moisture in the air is added to the atmosphere by evapotranspiration from the vast irrigated plains and forestlands (de Kok *et al.*, 2018; Harding *et al.*, 2013; Wei *et al.*, 2013; Tuinenburg *et al.*, 2012). Heavy precipitation events are encountered whenever these systems coincide and interact with each other (SUPARCO and FAO, 2010; WMO, 2010; Zaidi, 2014).

Precipitation distribution in the high-altitude Indus basin is extremely variable due to varying influence and interplay of the prevailing synoptic-scale atmospheric circulation systems with the local climate and topographic features. Highly sparse and directionally biased network of existing in situ observations insufficiently represents the entire range of a diverse climate in the study area (Fowler and Archer, 2006; Reggiani and Rientjes, 2015; Immerzeel *et al.*, 2015a; Dahri *et al.*, 2016; Dahri *et al.*, 2018). Hence, our understanding of the prevailing hydro-meteorological processes in this region is seriously uncertain (Andermann *et al.*, 2011; Lutz *et al.*, 2014).

Reliance on gridded data sets has been increased due to inadequate in situ observations and increasing demand for precipitation data in spatially distributed format. Therefore, a number of gridded precipitation products have been developed over the recent decades. Available data sets can broadly be categorized into four groups: gauge-based, reanalysis, satellite-derived and merged products. The gauge-based data sets are derived from the on-field direct measurements and provide relatively precise occurrences, amounts and types of precipitation at the measuring points. These point measurements are

often used for calibration, validation and bias correction of reanalysis and satellite estimates. However, the gauge-based precipitation data sets are also prone to observational uncertainties resulting from measurement errors, insufficient spatial and temporal coverage, uneven distribution and directional biases of the gauges, difficulties in snowfall measurements in windy conditions, and the applied interpolation methods. The magnitude of these uncertainties can be significant in orographically influenced mountain terrains (Lundquist *et al.*, 2010; Boers *et al.*, 2016; Prein and Gobiet, 2017; Dahri *et al.*, 2018).

Alternatively, several precipitation estimates modelled through Retrospective weather forecast model analysis (Reanalysis) or derived from satellite data provide gauge-independent estimates. These data sets offer viable substitutes for homogeneous, consistent, near-real-time and fairly reliable estimates of a wide range of climatic variables at global scale (Ghodichore *et al.*, 2018). A typical reanalysis system objectively integrates observations, a global forecast model, and an assimilation scheme to generate synthesized estimates of the past atmospheric states at global scale (Fujiwara *et al.*, 2017). Conversely, precipitation products derived from satellite data have gone through gradual improvements since their inception and currently incorporate data from several instruments and satellites (e.g., Huffman *et al.*, 2007; Joseph *et al.*, 2009; Ushio *et al.*, 2009; Xie *et al.*, 2017; Ciabatta *et al.*, 2018; Huffman *et al.*, 2018). Yet these products are poor in precisely capturing the solid precipitation (Rasmussen *et al.*, 2012; Putkonen, 2004). The satellite-based precipitation products vary considerably in terms of their source and processing algorithms as several sensors aboard geostationary earth orbiting (GEO) and low-earth orbiting (LEO) satellites observe precipitation passively or actively. A few studies observed that satellite-based products are better at estimating convective precipitation, whereas frontal system precipitation is better characterized by reanalysis (e.g., Ebert *et al.*, 2007; Ruane and Roads, 2007; Sapiano and Arkin, 2009; Tian *et al.*, 2009; Vila *et al.*, 2010). This indicates that reanalysis and satellite-derived data sets are complementary, particularly for the areas where validations are inadequate or impossible due to lack or absence of in situ observations (Peña-Arancibia *et al.*, 2013; Beck *et al.*, 2017).

Owing to the underlying issues in the available data sets to precisely estimate extreme heterogeneity of precipitation, several attempts have been made to take full advantage of the complementary nature and comparative advantages of the gauge-based observations, satellite data and reanalysis products. Numerous merged precipitation products have been developed over the recent time

(e.g., Xie and Arkin, 1997; Janowiak and Xie, 1999; Huffman *et al.*, 2007; Weedon *et al.*, 2014; Ashouri *et al.*, 2015; Funk *et al.*, 2015a, 2015b; Karger *et al.*, 2017; Xie *et al.*, 2017; Beck *et al.*, 2019). These data sets mostly rely on merging algorithms to limit the shortcomings of the source data sets and aim to produce higher quality end products.

Although, gridded data sets provide better information in terms of spatiotemporal consistency, their inadequacy to precisely estimate occurrence, quantity and type of precipitation is still a major concern. Recent innovations in weather forecasting models, satellite sensors and retrieval methods, and multi-source merging techniques coupled with high-quality observations have significantly improved the quality of resultant precipitation products. Yet, their spatiotemporal accuracy at basin/catchment scales particularly in orographically influenced and topographically diversified mountain terrains is highly variable (Maggioni *et al.*, 2016; Beck *et al.*, 2017; Henn *et al.*, 2018; Sun *et al.*, 2018; Beck *et al.*, 2019). There are also seasonal biases and difficulties in capturing the low intensity and snowfall events. Many existing precipitation products exhibit differences that are often larger than can be explained by observational or methodological uncertainties (Aghakouchak *et al.*, 2012; Yin *et al.*, 2015). Several evaluation studies have been undertaken at varying spatial scales using a variety of approaches, performance metrics and statistical indices (see reviews by Sun *et al.*, 2018; Maggioni *et al.*, 2016; and Gebremichael, 2010). However, inconsistency in terms of reference data set against which the accuracy is to be evaluated is an important issue. Many studies relied on spatially inconsistent point observations to assess the accuracy of gridded data sets; while others re-used many gauge observations already incorporated in development or validation of precipitation data sets, thereby precluding independent validation (Beck *et al.*, 2019). Even though it is well-recognized that the gauge observations are prone to significant measurement errors (Sevruk and Hamon, 1984; Legates and Willmott, 1990; Goodison *et al.*, 1998), these point-based gauge observations are often used without addressing uncertainties. Such reference point observations generally lack the required density to accurately represent the spatial heterogeneity of precipitation. Hydrological modelling is also used to evaluate quality of precipitation data by comparing observed and simulated flows obtained through varying precipitation inputs. However, the uncertainties associated with the modelling structure and other input data are the major drawbacks of this approach.

Performance of gridded precipitation products may often be satisfactory at global/continental scale, but they generally lack the accuracy and precision required at

sub-regional and catchment scale studies, especially over regions of high spatio-temporal heterogeneity (Gampe and Ludwig, 2017; Ghodichore *et al.*, 2018). The Indus river basin traversing through the high mountain ranges of the Tibetan Plateau (TP) and Hindukush-Karakoram-Himalaya (HKH) regions is experiencing significant transformations in its hydrometeorology (Lutz *et al.*, 2016) and is recognized as climate change hotspot (De Souza *et al.*, 2015; Lutz *et al.*, 2018; Krishnan *et al.*, 2019). There is no comprehensive study that evaluated performance of gridded data sets in this area. Few studies evaluated the performance of some gridded precipitation products against a limited number of point observations (e.g., Krakauer *et al.*, 2019; Ullah *et al.*, 2019; Ahmed *et al.*, 2019; Khan *et al.*, 2018; Iqbal *et al.*, 2018; Hussain *et al.*, 2017; Ali *et al.*, 2012) or against spatially distributed fields of mean annual precipitation derived from a limited number of point observations (e.g., Ghulami *et al.*, 2017; Anjum *et al.*, 2018). Dahri *et al.* (2016) integrated precipitation data from diverse sources to derive better estimates of spatially distributed precipitation and corroborated the underlying issues related to four important gridded precipitation products in this region. Others (e.g., Palazzi *et al.*, 2013; Reggiani and Rientjes, 2015) have relied on inter-comparison of a few data sets in the absence of reference data set.

This study therefore comprehensively and rigorously evaluates the applicability, robustness and limitations of 27 widely used precipitation products for the high-altitude Indus basin. The study is unique in that it assesses the performance and reliability of a wide range of products over a finer spatial scale. Quantitative and spatial variability of precipitation products is investigated at monthly, seasonal and annual scales against high-quality reference data set developed by Dahri *et al.* (2018). In addition, it cross validates the precipitation estimates of all gridded products using adjusted river flows through Turc-Budyko non-dimensional analysis. The study will provide useful inputs and guidelines for development, bias correction and improvement of gridded data sets. It will also serve as the basis for selection and use of appropriate data sets for hydrological and water assessment studies in the study area.

2 | DATA AND METHODS

2.1 | Reference data set

The accuracy of a product is usually assessed against a high-quality reference benchmark. Here we used a high-

resolution (≈ 1 km) data set of mean monthly precipitation recently developed by Dahri *et al.* (2018). This data set was derived by integration of several observational-based precipitation data sources with indirect estimates of precipitation from snow accumulations measured at the major glacier zones to cover the observational gaps. The precipitation observations were adjusted for measurement errors, net snow accumulations for the ablation losses, and observed river flows for the contribution of net glacier mass balance. Precipitation estimates at sub-basin scale were cross-validated by the corresponding adjusted specific runoff. The details on input data sets and techniques used in the development and cross-validation of the reference precipitation data set are comprehensively described in Dahri *et al.* (2018). Accuracy of the selected gridded precipitation products in this study is evaluated for each common grid cell with respect to this novel and high-resolution reference data set of mean monthly precipitation at basin and sub-regional scale.

2.2 | Gridded precipitation products

The selection of gridded data sets for this evaluation study is primarily based on availability of long-term (~ 20 years) records, which must coincide with the period of the reference data set (1999–2011). The three types of data evaluated in this study include gauge-based, reanalysis and merged precipitation products. We excluded the satellite-derived products due to their short-term records, which do not coincide with the reference period and their large uncertainty to estimate solid precipitation (Rasmussen *et al.*, 2012; Putkonen, 2004), which is dominant in the study area. The objective is to include all the important data sets. Therefore, an ensemble of 27 gridded precipitation products available for the historical periods is selected to evaluate their accuracy in the study area. The major characteristics of the selected data sets are summarized in Table 1. In a couple of cases, multiple versions are included to examine if the revision has actually improved the quality of newer version. For details on the input data sets and techniques used in their development, the corresponding references and concerned websites are suggested.

The data sets available at finer temporal resolutions were aggregated to monthly scale. Mean monthly precipitation climatologies for the reference period (1999–2011) for each gridded data set were then regridded to 30 arc-seconds (≈ 1 km at the equator) to precisely match the boundaries at sub-basin scale and spatial resolution of the reference data set using the conservative regridding method to preserve the original estimates of each gridded precipitation product. Extended winter (Oct–May) and

TABLE 1 Summary of the basic characteristics of the selected gridded precipitation products for this study

S. #	Product Name and Details	Data Source	Grid Size	Temporal Coverage	Reference
Gauge-based Products					
1	GPCC V8, Global Precipitation Climatology Centre (GPCC) Full Data Monthly Product Version 8	G	0.25°	1891-2016	Schneider et al. (2018)
2	GPCC V7, Global Precipitation Climatology Centre (GPCC) Full Data Monthly Product Version 7	G	0.5°	1901-2013	Schneider et al. (2014)
3	UDEL V5.01, University of Delaware, Terrestrial Precipitation: Gridded Monthly Time Series (V 5.01)	G	0.5°	1900-2017	Mats. & Willm. (2018)
4	APHRODITE V1801R1, Asian Precipitation - Highly-Resolved Observational Data Integration Towards Evaluation V1801R1	G	0.25°	1998-2015	Yatagai et al. (2018)
5	APHRODITE V1101, Asian Precipitation - Highly-Resolved Observational Data Integration Towards Evaluation V1101	G	0.25°	1951-2015	Yatagai et al. (2012)
6	PREC-Land, NOAA's PRECipitation REConstruction over Land (PREC/L)	G	0.5°	1948-2012	Chen et al. (2002)
7	CRU TS4.02, Climate Research Unit TS4.02	G	0.5°	1901-2017	Harris et al. (2014)
8	GPCP V2.3, Global Precipitation Climatology Project (GPCP) Version 2.3 Monthly Analysis	G	2.5°	1979-NRT	Adler et al. (2018)
9	CPC Unified, Climate Prediction Center Unified gauge-based analysis V1.0	G	0.5°	1979-NRT	Chen et al. (2008)
Reanalyses Products					
1	ERA5, ECMWF's 5th generation Atmospheric ReAnalysis	R	~0.281°	1979-NRT	Hersbach et al. (2018)
2	CFSR, National Centers for Environmental Prediction (NCEP) Climate Forecast System Reanalysis	R	~0.31°	1979-2010	Saha et al. (2010)
3	JRA-55, Japanese 55-year ReAnalysis	R	0.5625°	1958-NRT	Kobayashi et al. (2015)
4	ERA 20C, ECMWF Atmospheric Reanalysis of the 20th Century	R	~1.406°	1900-2010	Stickler et al. (2014)
5	MERRA-2, Modern-Era Retrospective analysis for Research and Applications, Version 2	R	0.5°	1980-NRT	Gelaro et al. (2017)
6	ERA1, European Centre for Medium-range Weather Forecasts ReAnalysis Interim	R	~0.75°	1979-NRT	Dee et al. (2011)
7	DOE-R2, NCEP-Department of Energy (DOE) Reanalysis 2	R	~1.875°	1979-NRT	Kanamitsu et al. (2002)
8	NCAR-R1, NCEP-National Center for Atmospheric Research (NCAR) Reanalysis 1	R	~1.875°	1948-NRT	Kalnay et al. (1996)
9	20CR V2C, NOAA-CIRES Twentieth Century Reanalysis Version 2C	R	~1.875°	1851-2011	Compo et al. (2011)
Merged (combined gauge, reanalyses, satellite) Products					
1	MSWEP V2.2, Multi-Source Weighted-Ensemble Precipitation Version 2.2	G, S, R, A	0.1°	1979-NRT	Beck et al. (2017, 2019)
2	TMPA 3B42 V7, TRMM Multi-satellite Precipitation Analysis (TMPA) 3B42 V7	G, S	0.25°	1998-NRT	Huffman et al. (2007)
3	PERSIANN-CDR V1R1, Precipitation Estimation from Remotely Sensed Information using Artificial Neural Networks-Climate Data Record V1R1	G, S	0.25°	1983-2016	Ashouri et al. (2015)
4	CHELSA V1.2, Climatologies at High resolution for the Earth Land Surface Areas, Version 1.2	G, R, A	0.0083°	1979-2013	Karger et al. (2017)
5	CHIRPS V2.0, Climate Hazards group Infrared Precipitation with Stations Version 2.0	G, S, R, A	0.05°	1981-NRT	Funk et al. (2015)
6	WFDEL-CRU, WATCH Forcing Data ERA-Interim corrected by CRU	G, R	0.5°	1979-2015	Weedon et al. (2014)
7	CMAP, CPC Merged Analysis of Precipitation	G, S, R	2.5°	1979-NRT	Xie and Arkin (1997)
8	CMORPH V1.0, CPC MORPHing technique (CMORPH) V1.0	G, S	0.5°	1998-NRT	Xie et al. (2017)
9	CAMSOP1, Climate Anomaly Monitoring System ("CAMS") and OLR Precipitation Index ("OPI")	G, S	2.5°	1979-NRT	Janowiak & Xie (1999)

monsoon (Jun–Sep) seasons are regarded keeping in view the onset and continuity of precipitation during the two major circulation systems (winter westerlies and summer monsoon) prevailing in the study area.

2.3 | River flows

Dahri *et al.* (2018) collected river flow data for all major sub-basins in the study area and accounted for the diversions upstream of each river gauge. These observed river flows were adjusted for the contributions of net mass balances using mass balance estimates provided by Käb *et al.* (2015, Käb *et al.*, 2012) and glacier areas estimated by Randolph Glacier Inventory (RGI) version 5.0 (Arendt *et al.*, 2015). These adjusted river flows are used in this study for cross validation of the precipitation from the selected products through Turc-Budyko non-dimensional analysis.

2.4 | Potential evapotranspiration

There is no observational-based independent data set of potential evapotranspiration (PET) for the study area. Therefore, previous studies have relied on global-scale

gridded data sets using PET data from a single product (e.g., Dahri *et al.*, 2018) or ensemble mean of several data sets (e.g., Immerzeel *et al.*, 2015b). Importantly, PET does not have critical use in this study. It is only required to estimate aridity index (P/PET) in Turc-Budyko non-dimensional analysis. Recently, a fifth generation reanalysis (ERA5) data set with numerous atmospheric variables at global scale has been released. The evaluation of precipitation products undertaken in this study reveals that precipitation estimates of ERA5 are better than the rest of data sets for the study area. Therefore, as a complementary climate variable, PET from ERA5 reanalysis is selected for this study.

2.5 | Evaluation approach

The study area is stretched over vast mountain and sub-mountain ranges of extremely variable topographic features in the Indus basin. The confluence of Hindukush-Karakoram-Himalayan mountain ranges adds significant complexities in characterizing the connection between precipitation and topographic features (Palazzi *et al.*, 2013). These three mountain ranges are influenced differently by the underlying atmospheric circulation systems and possess unique hydrometeorological and

geomorphological characteristics. Therefore, in order to have a better idea of the quality of spatial distribution depicted by various gridded precipitation products and based on the availability of observed streamflows for ultimate evaluation and cross validation; the study area is divided into five sub-regions (Figure 1), which possess unique differences in their precipitation patterns and magnitudes, and landscape morphologies.

Widely used statistical measures and quantitative analysis techniques are used to evaluate performance of the selected gridded precipitation products. All analyses are performed on the common grids for the reference period of 1999–2011. Mean annual precipitation for the reference period over the study area is plotted for each gridded data set to visually examine their spatial distribution. The biases between mean annual precipitation of each gridded data set and the corresponding grid of the reference data set are plotted to show the spatial distribution of their residuals over the study area. The biases between mean monthly precipitation of each gridded data set and reference data set at each corresponding grid are analysed through Box-Whisker charts for extended winter (Oct–May) and monsoon (Jun–Sep) seasons, which are further extended at annual scale for the study area as well as its five sub-regions to examine their median, distribution and spread at first and third quarters and extremes. This is followed by computation of mean absolute error (MAE) in mean monthly precipitation of all gridded data sets against the reference data set. The MAE computes the magnitude of the mean differences between two data sets without considering the direction of the error and is given by Equation (1). The MAE is generally a preferred metric over widely used root mean square error (RMSE) when the errors are unlikely to follow a normal distribution (Chai and Draxler, 2014; Beck *et al.*, 2017; Willmott *et al.*, 2017).

Modified Kling-Gupta Efficiency (KGE) scores are computed using Equation (2) (Gupta *et al.*, 2009; Kling *et al.*, 2012) at monthly and annual scale for the study area and at annual scale for the five sub-regions to examine how closely the spatio-temporal precipitation estimates of the gridded data sets are statistically matched with those of the reference data set. Any value of KGE gives the lower limit of its three components, meaning that the worst component is \geq to that value. The KGE has primarily been used for evaluating the quality of climate or hydrological models' outputs against the observed data. However, it can also be used to evaluate the performance of gridded precipitation products against the corresponding reference data (Beck *et al.*, 2019). The mathematical expressions of the employed performance evaluation metrics are given by:

$$\text{MAE} = \frac{1}{n} + \sum_{i=1}^n |G_i - R_i| \quad (1)$$

$$\text{KGE} = 1 - \sqrt{(r-1)^2 + (\beta-1)^2 + (\gamma-1)^2} \quad (2)$$

$$r = \frac{\sum_{i=1}^n (G_i - \bar{G})(R_i - \bar{R})}{\sqrt{\sum_{i=1}^n (G_i - \bar{G})^2 \sum_{i=1}^n (R_i - \bar{R})^2}} \quad (3)$$

$$\beta = \frac{\mu_{\text{grd}}}{\mu_{\text{ref}}} \quad (4)$$

$$\gamma = \frac{\sigma_{\text{grd}}/\mu_{\text{grd}}}{\sigma_{\text{ref}}/\mu_{\text{ref}}} \quad (5)$$

Where: G_i and R_i represent the gridded and reference data sets at i_{th} grid and n denotes number of grid cells, r in Equation (2) is Pearson's correlation coefficient to measure the degree of linear relation between two data sets, β is bias computed by the ratio of gridded and reference means (μ), γ is variability ratio given by the ratio of the gridded and reference data set's coefficients of variation (σ/μ), σ is standard deviation, and subscripts $_{\text{grd}}$ and $_{\text{ref}}$ indicate gridded and reference data sets respectively. The optimum values of KGE, r , β and γ are at unity.

For robust quantitative assessment, the study further evaluated the annual cycle of area-weighted mean monthly precipitation of each gridded data set for the reference period against that of the reference data set. This comparison evaluates how well the gridded data sets follow the mean monthly and seasonal cycle of precipitation during the reference period in the study area and in each sub-region. The goodness-of-fit of these monthly cycles is ascertained through coefficient of determination (R^2) and MAE.

Isolated measures of performance evaluation are often associated with their specific uncertainties and limitations resulting in contrasting inferences. Therefore, instead of relying on a single measure, the outcomes of the above-described performance metrics are integrated through a simple ranking system to evaluate the performance of the gridded data sets in a better and more consistent manner. For this purpose, the originally estimated values of these performance metrics for each gridded data set are normalized and rescaled between 0 and 1. However, in contrast to KGE and R^2 , lower values of MAE infer better performance. Therefore, the normalized values of MAE are subtracted from one to synchronize them with KGE and R^2 . The integrated skill scores are obtained by sum of the normalized values of KGE and R^2 and subtracted normalized values of MAE for each data set. The larger values infer higher rankings. This simple

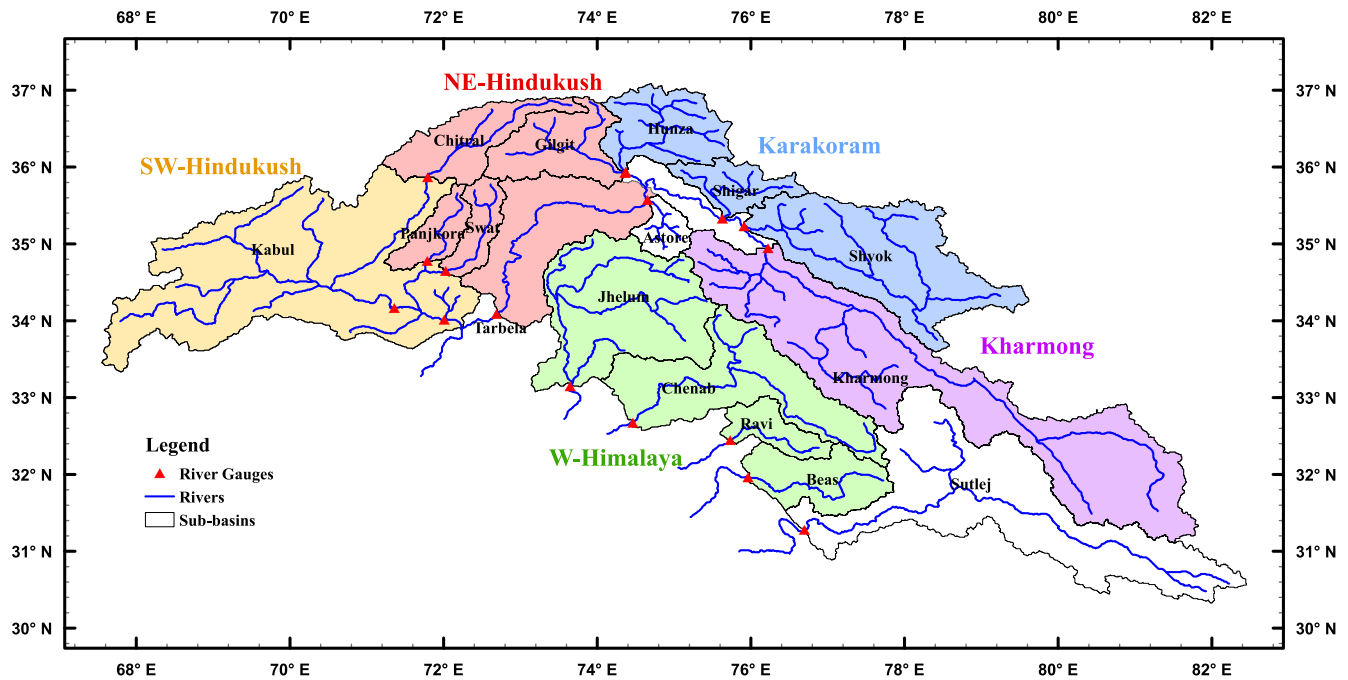


FIGURE 1 Study area and location of five regions analysed in this study [Colour figure can be viewed at wileyonlinelibrary.com]

ranking system greatly reduces the contradictions and complexities in interpretation of the evaluation results. Furthermore, the wet and dry areas are defined by combining the sub-regions where annual mean precipitation is more and less than 600 mm, respectively. Hence, the wet area adds the skill scores of W-Himalaya, Karakoram and NE-Hindukush, while dry area combines Kharmonig and SW-Hindukush sub-regions. Similarly, the rankings and skill scores are also calculated for Indus basin upstream of Tarbela dam (Figure S1 and Table S3).

Finally, the mean annual precipitation estimates of all data sets are cross-validated by the corresponding adjusted streamflows (specific runoff) using Turc-Budyko non-dimensional analysis (Turc, 1954; Budyko, 1974; Valéry *et al.*, 2010; Andréassian and Perrin, 2012). Adjusted river flows determined in Dahri *et al.*, 2018, potential evapotranspiration (PET) from ERA5 reanalysis product and precipitation estimates of gridded data sets for the whole study area and five sub-regions are used to compute run-off ratio (Q/P) and aridity index (P/PET). The Turc-Budyko non-dimensional analysis approach was originally introduced by Turc (1954) and Budyko (1974) to represent the relationships between actual and potential evapotranspiration (AET/PET) and between precipitation and potential evapotranspiration (P/PET). However, actual evapotranspiration is difficult to measure and spatially distributed data are very rare and often highly biased. Therefore, it was later on modified and further elaborated by an equivalent and alternative representation

between Q/P and P/PET and introducing water and energy limits (e.g., Valéry *et al.*, 2010; Andréassian and Perrin, 2012; Coron *et al.*, 2015). Since then, the approach has been extensively applied in hydrometeorological and water balance assessments in several regions. The rankings and integrated skill scores of the data sets for each region are recognized only if a particular data set falls within the theoretically feasible domain of Q/P ratio in Turc-Budyko representation. The order of the ranking is updated accordingly after exclusion of the underperforming data sets in this criterion.

3 | RESULTS

3.1 | Spatial distribution of mean annual precipitation and residual errors

Spatial distribution of mean annual precipitation estimates from various gridded data sets presented in Figure 2a and area-weighted seasonal and annual precipitation totals provided in Table 2 reveal significant variability of mean annual precipitation. Compared to annual mean precipitation of 697 mm of the reference data set, the minimum estimates of 374 mm (−46%) are depicted by CPC Unified and maximum estimates of 976 mm (+40%) by ERAI data sets. However, the magnitudes vary considerably at sub-regional and seasonal scale. None of the selected gridded precipitation products could accurately distinguish and capture the

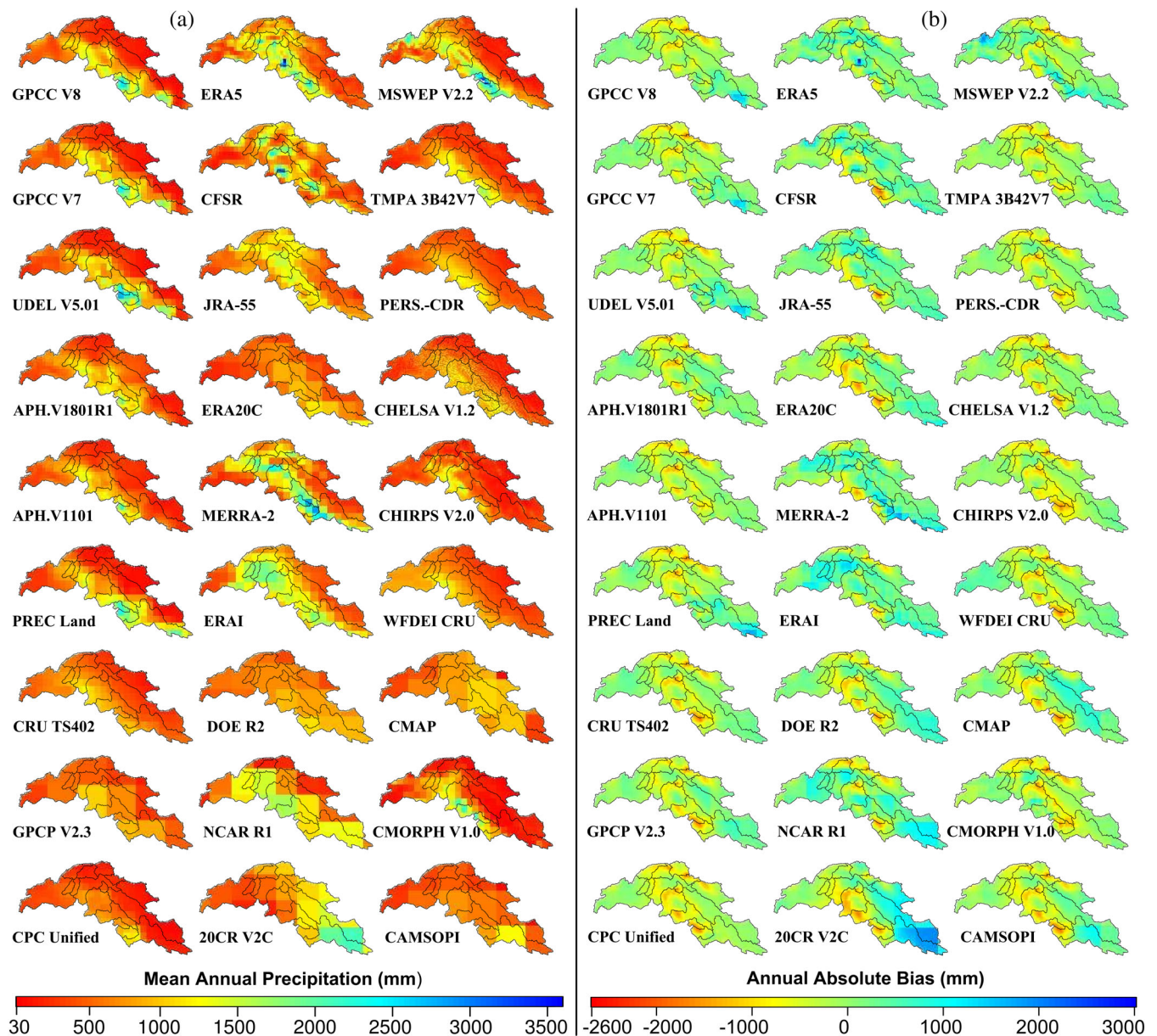


FIGURE 2 Spatial distribution of (a) mean annual precipitation illustrated by various gridded data sets, and (b) absolute bias (difference) between mean annual precipitation of these gridded products with respect to the reference data set (Figure 3m in Dahri *et al.*, 2018). In both (a) and (b) pannels, left column shows gauge-based products, middle column shows reanalyses and right column shows the merged products [Colour figure can be viewed at wileyonlinelibrary.com]

zone of second precipitation maxima present in the central Karakoram. All gridded data sets also failed to detect the drier areas under the influence of rain shadows. However, significant consistency in terms of spatial patterns showing negative or dry bias in wet areas and positive or wet bias in dry areas with considerable difference in the magnitude of biases is noticed. Most prominent are the two swaths/paths of negative bias: first from upper Chitral basin and passing through Gilgit, Hunza, Shigar and Shyok basins; and second along the western Himalayan foothills from

Beas across Chitral sub-basin. A large spread of residual errors (ranging from $-2,600$ to $3,000$ mm) with respect to the reference data set (Figure 2b) is also evident.

The gauge-based and merged products show strong tendency of underestimation; while all reanalysis products, except ERA20C, tend to overestimate precipitation in most parts of the study area, with considerable differences at sub-regional level. This overestimation by the reanalysis products is more pronounced in the drier areas (e.g., Khar Mong and SW-Hindukush). With the exception

TABLE 2 Area-weighted seasonal and annual precipitation estimates by the reference data set and percent difference in the precipitation estimates of various gridded data sets

S. Precipitation # Product	Study Area			W-Himalaya			Karakoram			Kharmonig			NE-Hindukush			SW-Hindukush		
	O - M	J - S	ANN	O - M	J - S	ANN	O - M	J - S	ANN	O - M	J - S	ANN	O - M	J - S	ANN	O - M	J - S	ANN
0 REFERENCE (mm)	457.7	239.6	697.3	778.7	584.2	1362.9	434.7	187.3	622.0	210.4	73.6	284.0	628.7	246.4	875.1	350.5	87.0	437.5
1 GPCC V8	-23.9	12.0	-11.6	-29.8	5.3	-14.7	-73.8	-76.3	-74.5	-6.9	42.5	5.9	-40.3	-13.2	-32.7	11.3	72.6	23.5
2 GPCC V7	-24.2	11.9	-11.8	-30.7	4.1	-15.8	-73.7	-76.2	-74.4	-2.4	51.4	11.5	-41.3	-14.6	-33.8	11.3	72.4	23.5
3 UDEL V5.01	-18.6	9.4	-9.0	-22.1	6.8	-9.7	-72.3	-76.8	-73.6	27.8	73.6	39.6	-48.7	-24.8	-42.0	3.3	20.3	6.7
4 APH.V1801R1	-27.0	9.4	-14.5	-36.2	-11.4	-25.5	-48.3	-31.6	-43.3	15.4	164.9	54.1	-42.5	-20.5	-36.3	11.2	80.3	25.0
5 APH.V1101	-37.3	-7.0	-26.9	-43.5	-21.2	-33.9	-62.3	-59.5	-61.5	-28.4	61.4	-5.1	-41.4	-19.8	-35.4	7.6	70.5	20.1
6 PREC Land	-32.3	33.0	-9.9	-41.2	20.1	-14.9	-82.3	-72.6	-79.4	-14.5	113.2	18.6	-50.2	-0.9	-36.3	-4.2	48.0	6.2
7 CRU TS402	-36.9	1.4	-23.8	-59.6	-22.7	-43.8	-57.7	-76.5	-63.4	-15.0	127.9	22.0	-34.1	-4.1	-25.7	21.1	103.8	37.6
8 GPCP V2.3	-40.1	22.6	-18.5	-57.1	-13.3	-38.3	-51.2	-25.8	-43.6	-6.4	306.7	74.7	-43.9	-19.8	-37.1	-12.1	64.0	3.0
9 CPC Unified	-59.9	-20.5	-46.4	-63.9	-28.7	-48.8	-76.4	-64.7	-72.8	-56.5	24.9	-35.4	-62.6	-44.1	-57.4	-26.5	57.5	-9.8
1 ERA5	6.9	42.9	19.3	-0.6	10.6	4.2	-7.3	12.4	-1.4	17.6	196.1	63.8	8.5	43.1	18.3	29.4	143.7	52.2
2 CFSR	19.1	-3.8	11.2	-12.7	-27.3	-18.9	39.7	-9.9	24.8	85.6	177.4	109.4	14.0	-34.2	0.4	16.7	-5.3	12.3
3 JRA-55	18.2	19.9	18.8	-10.6	-26.2	-17.3	51.3	-8.1	33.4	53.9	270.7	110.1	13.5	-10.6	6.7	25.3	131.1	46.4
4 ERA 20C	-31.3	12.5	-16.2	-53.9	-26.2	-42.0	-42.7	-14.5	-34.2	43.3	277.3	103.9	-34.6	-43.3	-37.0	-29.4	-18.2	-27.1
5 MERRA-2	11.9	74.0	33.2	-1.8	18.6	7.0	20.4	3.4	15.3	21.2	287.1	90.1	9.7	64.6	25.1	28.6	75.9	38.0
6 ERAI	20.9	76.5	40.0	-3.4	8.6	1.7	-20.9	3.7	-13.5	60.0	260.3	111.9	37.7	115.2	59.5	52.9	261.3	94.3
7 DOE R2	2.1	-3.3	0.2	-35.3	-42.9	-38.6	-4.0	-48.2	-17.3	141.4	253.3	170.4	-22.0	-46.8	-29.0	15.0	56.8	23.3
8 NCAR R1	34.4	30.1	32.9	7.4	-21.2	-4.9	-58.1	-33.7	-50.8	163.2	331.7	206.8	35.9	-26.7	18.3	60.1	222.2	92.3
9 20CR V2C	10.1	80.1	34.1	-55.6	-38.5	-48.3	78.8	48.2	69.6	187.5	547.3	384.4	-18.7	-76.9	-35.1	5.1	-89.8	-13.8
1 MSWEP V2.2	-7.9	39.4	8.3	-23.0	30.3	-0.1	-60.8	-63.7	-61.7	-31.2	67.7	-5.6	-0.6	21.8	5.7	76.8	81.6	77.8
2 TMPA 3B42 V7	-44.1	9.6	-25.6	-47.0	-4.4	-28.8	-68.2	-44.8	-61.1	-32.0	109.4	4.6	-51.2	-7.5	-38.9	-21.7	48.9	-7.6
3 PERS-CDR V1R1	-40.3	13.6	-21.8	-54.8	-6.6	-34.2	-51.1	-50.2	-50.8	-20.6	191.0	34.2	-41.1	-0.9	-29.8	-11.0	69.8	5.1
4 CHLSA V1.2	-31.8	-13.6	-25.6	-39.8	-27.1	-34.3	-66.0	-60.5	-64.3	-0.2	53.5	13.7	-40.0	-28.6	-36.8	-5.0	23.0	0.6
5 CHIRPS V2.0	-47.5	-17.5	-37.2	-61.1	-27.3	-46.6	-65.8	-62.6	-64.9	-38.7	45.0	-17.0	-43.1	1.1	-30.7	-2.3	-9.9	-3.8
6 WFDEI-CRU	-28.9	3.8	-17.7	-58.9	-26.5	-45.0	-49.4	-78.9	-58.3	-6.8	115.1	24.8	-26.5	0.8	-18.8	52.5	198.7	81.6
7 CMAP	-7.1	23.3	3.4	-42.8	-27.5	-36.2	39.7	-3.6	26.7	128.1	295.7	171.5	-19.9	-33.4	-23.7	-14.6	81.4	4.5
8 CMORPH V1.0	-52.4	-3.1	-35.5	-40.9	-16.7	-30.5	-92.7	-56.9	-81.9	-64.5	-0.1	-47.8	-54.3	32.0	-30.0	-28.2	128.6	3.0
9 CAMSOP1	-55.5	43.9	-21.4	-69.0	-22.8	-49.2	-62.7	18.6	-38.2	-31.4	414.0	84.0	-53.2	-30.6	-46.9	-33.8	60.2	-15.1

Note: The graduated colour scheme highlights the changes as per grid cell values.

of a few reanalysis products (e.g., ERA5, CFSR, JRA-55, MERRA-2 and 20CR), the largest underestimates of gridded data sets are observed in the Karakoram region. Interestingly, DOE R2 provides the best quantitative estimate at basin scale but its quantitative estimates, correlations and KGE scores at sub-regional scale are below par. The inter-regional variations are offset when aggregated for the whole study area. This underlines the importance of consistency in accuracy of precipitation estimates at varying spatial scales.

3.2 | Residual errors

Residual errors in mean monthly precipitation of the gridded data sets summarized in Figure 3 suggest large deviations from the reference mean. However, the errors vary considerably among the data sets at seasonal scale and over the sub-regions. The largest spreads of residual errors are found in W-Himalayan region for all products, partly due to highest precipitation. The gauge-based and merged products perform relatively better during monsoon season and reanalysis products during the winter months. Generally, reanalysis products show larger variability and wider

spread of residuals than gauge-based and merged products, which is understandable and attributed to their independence from direct measurements of precipitation, use of varying type and number of assimilated observations, and use of different atmospheric models and assimilation schemes. The gauge-based and merged products significantly underestimate precipitation in relatively wet regions of W-Himalaya, NE-Hindukush and Karakoram. None of the selected products could be singled out as the best product for all regions as their accuracy varies considerably from one region to another. However, ERA5, GPCC V8 and MSWEP2.2 provide better estimates among their counterpart grouped products.

Mean absolute error (MAE) magnitudes of the gridded data sets (Figure 4) depict almost similar patterns of the errors as in Figure 3. The largest MAEs are observed in W-Himalayan region and during monsoon season. Gauge-based products show relatively small absolute errors except higher-altitude Karakoram region, where reanalysis products perform much better. However, reanalysis products show larger errors during monsoon season, probably due to the convective nature of monsoon precipitation and high uncertainties in deep convection parameterization schemes applied in the

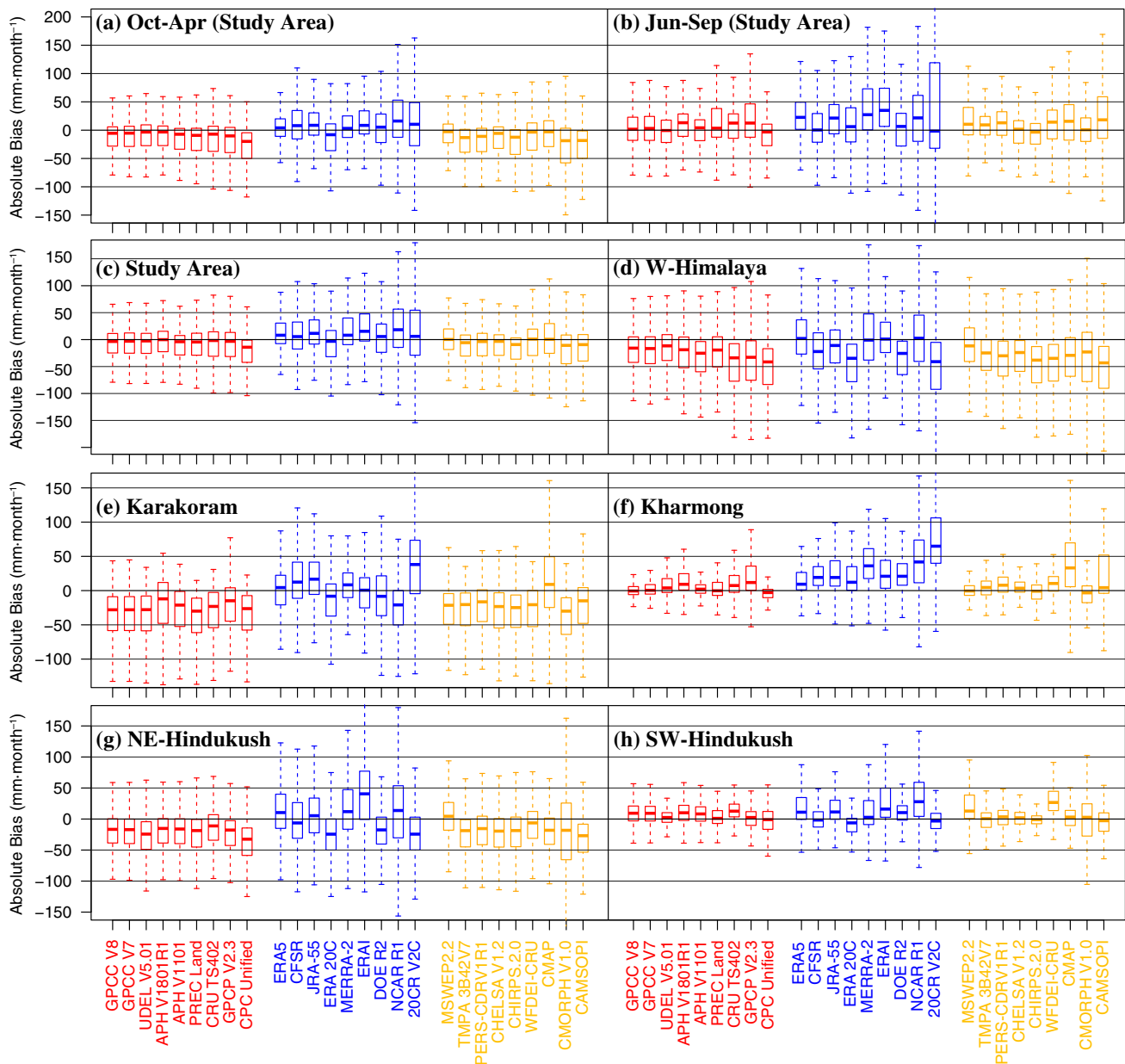


FIGURE 3 Box-whisker plots of the absolute bias of mean monthly precipitation of each gridded data set against the reference data set for Oct-may months and monsoon (Jun-Sep) season for the study area and extended at annual scale for the study area and its five regions. Red colour indicates data sets developed from gauge observations, blue colour represents reanalyses products and orange colour are the merged data sets. The zero line represents the mean precipitation of reference data set, the thick lines in the middle of boxes show the median differences, the bottom and top edges of the box represent the deviations from the reference mean at 25th and 75th percentiles respectively, while the 'whiskers' represent the extreme values for each gridded data set. Outliers are removed [Colour figure can be viewed at wileyonlinelibrary.com]

reanalysis models, which is in line with the findings of Beck *et al.* (2019). ERA5 is found best during winter and pre-monsoon (Oct–May) months and in higher-altitude Karakoram region, while GPCC V8 provides the least MAE values in W-Himalaya and Khar mong, WFDEI-CRU in NE-Hindukush, and CHIRPS V2.0 in SW-Hindukush regions.

3.3 | KGE scores

Very low to moderately high KGE scores ranging from -0.76 to 0.80 for various months (Figure 5a) and from -2.91 to 0.86 for various regions (Figure 5b) indicate very poor to moderately good performance of gridded data sets to match the precipitation pattern and magnitudes of the

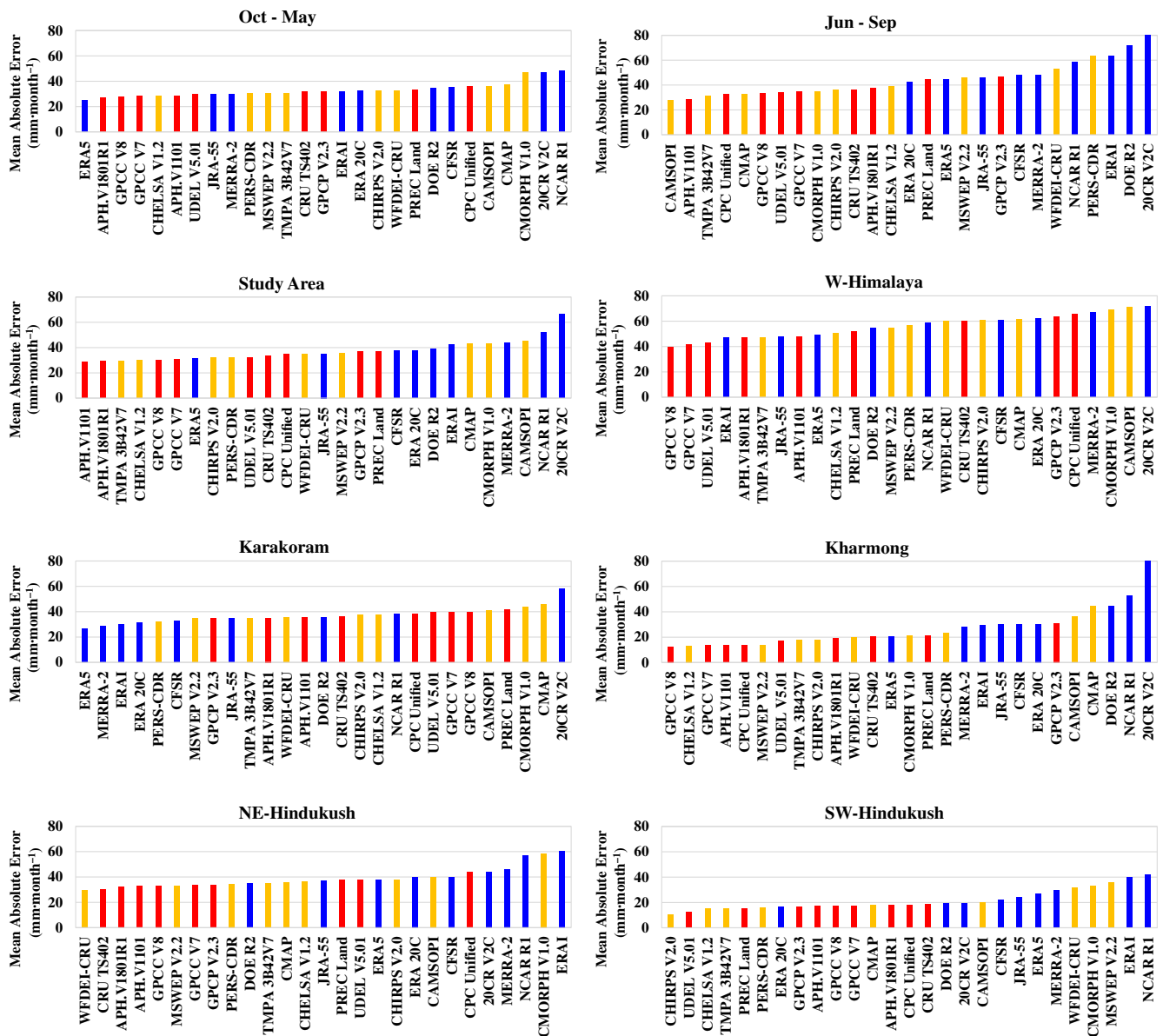


FIGURE 4 Mean absolute errors with the same group colour schemes and spatiotemporal scales as in Figure 3, but ranked according to error magnitudes [Colour figure can be viewed at wileyonlinelibrary.com]

reference data set. Negative KGE values reflect negative correlation and/or large deviation of bias and variability ratio from their optimum values. Except for ERA5, CFSR, JRA-55, MERRA-2 and ERAI; all other data sets provide lowest KGE scores during winter (Oct-Mar) months. ERA5 outperforms all data sets during Feb-May, while MERRA2 better performs during Oct-Jan. The gauge-based and few merged products depict better KGE scores during monsoon season (Jun-Sep). In case of extended monthly data at annual scale for the whole study area (Figure 5b), GPCC V8 produces the highest KGE score of 0.674 followed by GPCC V7 (0.673), MSWEP2.2 (0.634), UDEL5.01 (0.633), TMPA 3B42V7 (0.630), APHRODITE V1801R1 (0.617), APHRODITE V1101 (0.613) and ERA5 (0.590). However, KGE scores vary considerably at sub-regional level. GPCC V8 outperforms all the data sets in W-Himalaya and

Kharhong, MERRA-2 in Karakoram, MSWEP2.2 in NE-Hindukush, and CHIRPS V2.0 in SW-Hindukush regions. Details of monthly scale KGE scores, correlations, biases and variability ratios for the study area are provided in Table S1, while Table S2 presents the same metrics for extended time scale for study area and five sub-regions. The low KGE scores in Karakoram region can be attributed to greater topographical variability and larger spatio-temporal heterogeneity of precipitation in this high-mountain region.

3.4 | Annual cycle of monthly means

The observational-based reference climatologies of area-weighted mean monthly precipitation exhibit a strong seasonality with bimodal pattern clearly reflecting the

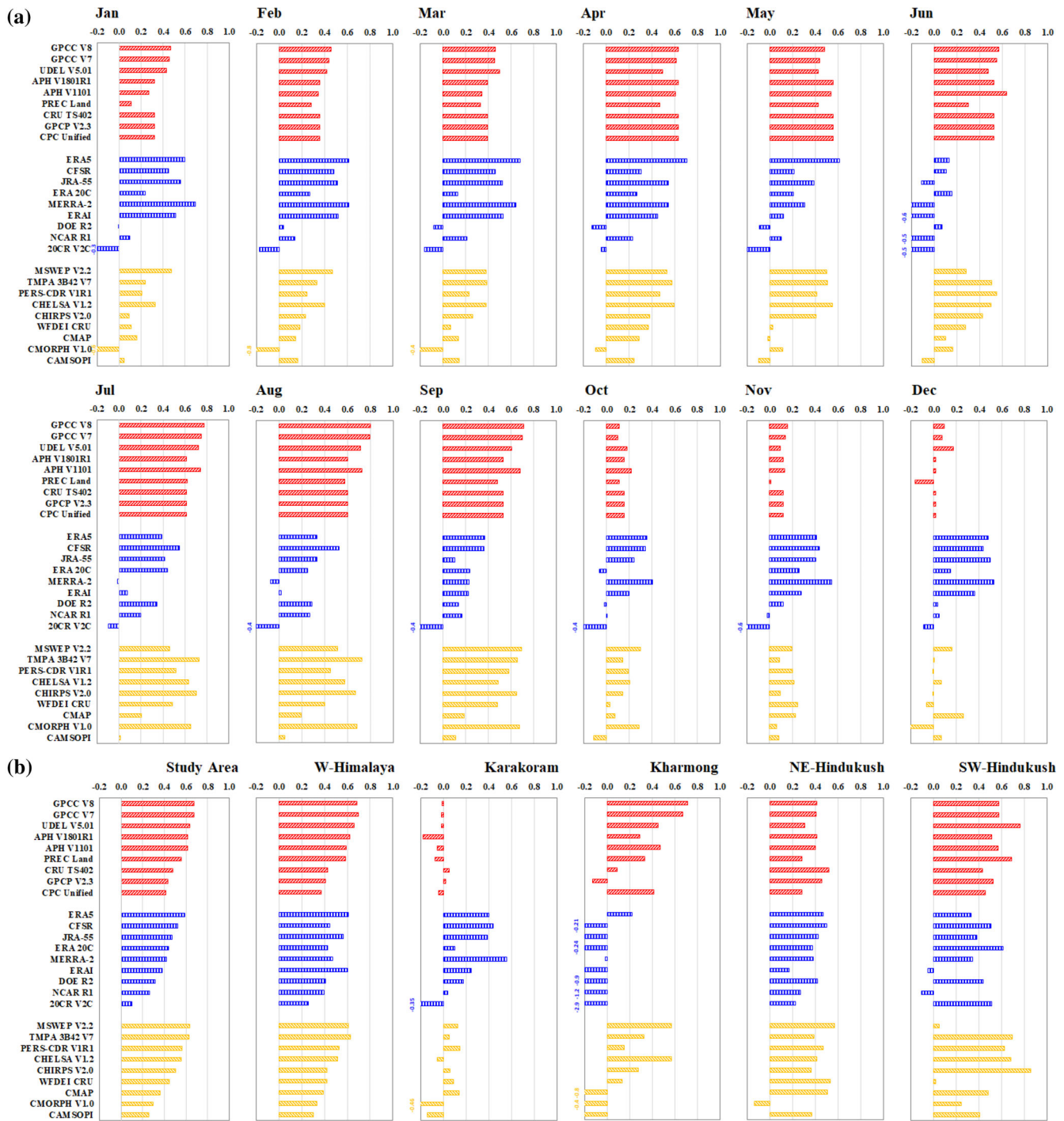


FIGURE 5 KGE scores based on mean monthly precipitation totals at monthly scale for the study area (a), and extended at annual scale for the study area and five regions (b). The red, blue and orange colours represent KGE scores for gauge-based, reanalyses and merged data sets, respectively [Colour figure can be viewed at wileyonlinelibrary.com]

influence of winter westerlies and summer monsoon, but many gridded data sets have difficulties in efficiently reproducing this seasonality and bimodal pattern as shown in Figure 6. Few data sets show very weak seasonality, and CMORPH even displays a 'negative' correlation. The strength of gridded products to reproduce the annual cycle of area-weighted mean monthly precipitation of the reference data set is ascertained by R^2 and MAE

(Table 3). Correlation coefficient and R^2 primarily indicate patterns and linear trend between two data but lack in quantifying the margin of errors, which is determined by MAE. None of the data set is equally best for all sub-regions due to a large variability in R^2 and MAE values.

All gauge-based products underestimate precipitation during Oct–May in all sub-regions except relatively dry sub-region of SW-Hindukush. They show mix trends

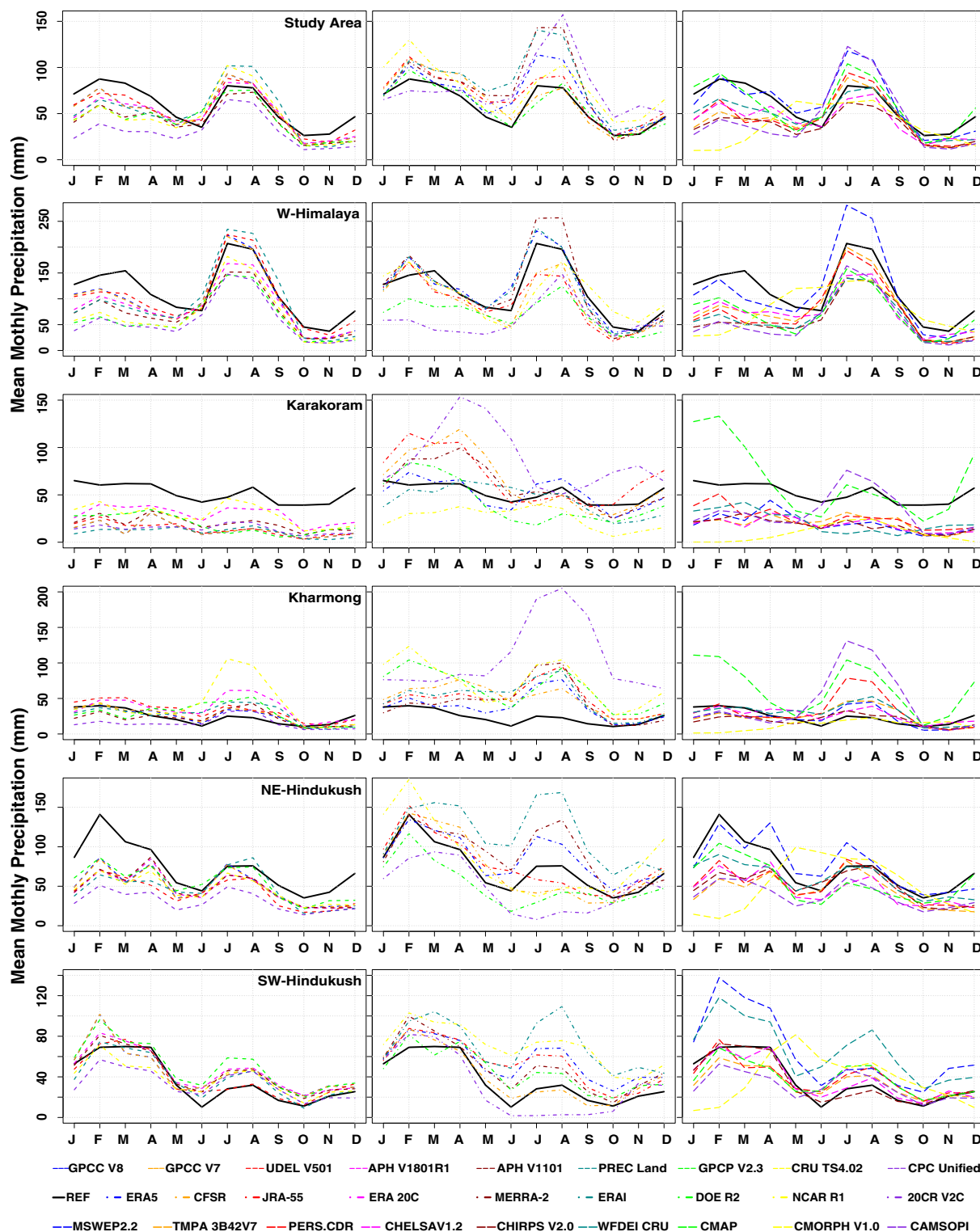


FIGURE 6 Annual cycle of mean monthly precipitation for the study area and five regions. Each row represents a particular region. Left column shows gauge-based data sets, middle column indicates reanalyses products and right column shows merged products [Colour figure can be viewed at wileyonlinelibrary.com]

during monsoon season with PREC Land, UDEL V5.01 and two versions of GPCC slightly overestimating precipitation in W-Himalaya, Kharmonig and SW-Hindukush regions. However, in the higher-altitude regions of

Karakoram and NE-Hindukush, the gauge-based products significantly underestimate precipitation throughout the year. An important discrepancy in attainment of the lowest and highest peaks is also evident. Almost all

TABLE 3 Coefficient of determination (R^2) and MAE (mm) values based on area-weighted monthly means presented in Figure

S. Precipitation # Product	Study Area		W-Himalaya		Karakoram		Khar Mong		NE-Hindukush		SW-Hindukush	
	R^2	MAE	R^2	MAE	R^2	MAE	R^2	MAE	R^2	MAE	R^2	MAE
1 GPCC V8	0.776	11.5	0.888	22.3	0.373	38.6	0.623	6.1	0.656	24.4	0.739	12.1
2 GPCC V7	0.769	11.6	0.886	22.6	0.369	38.6	0.611	6.7	0.650	25.0	0.738	12.1
3 UDEL V5.01	0.847	9.0	0.902	17.7	0.561	38.2	0.713	10.6	0.723	30.6	0.937	4.5
4 APH.V1801R1	0.725	12.2	0.872	30.7	0.264	22.4	0.189	14.9	0.581	26.5	0.889	9.7
5 APH.V1101	0.706	16.2	0.853	39.1	0.339	31.9	0.151	9.2	0.579	25.8	0.904	8.2
6 PREC Land	0.527	18.9	0.739	36.5	0.195	41.2	0.128	11.0	0.332	28.5	0.877	6.3
7 CRU TS402	0.553	16.9	0.665	52.0	0.573	32.8	0.018	14.3	0.665	20.1	0.829	13.7
8 GPCP V2.3	0.468	19.8	0.736	44.5	0.289	22.6	0.011	22.4	0.643	27.1	0.732	9.8
9 CPC Unified	0.472	27.0	0.732	55.4	0.204	37.8	0.051	11.7	0.672	41.8	0.622	12.3
1 ERA5	0.824	11.5	0.888	15.9	0.577	9.2	0.144	15.6	0.834	14.8	0.779	19.0
2 CFSR	0.839	10.0	0.854	25.7	0.546	19.5	0.308	25.9	0.760	15.5	0.909	7.3
3 JRA-55	0.894	11.0	0.757	25.6	0.632	19.9	0.073	26.1	0.820	13.5	0.743	16.9
4 ERA 20C	0.596	14.5	0.788	47.7	0.351	18.0	0.073	24.6	0.887	27.0	0.865	10.5
5 MERRA-2	0.685	21.0	0.926	20.8	0.493	14.8	0.020	24.1	0.622	21.4	0.886	13.8
6 ERAI	0.662	24.0	0.899	16.4	0.198	12.8	0.115	26.5	0.437	43.4	0.422	34.4
7 DOE R2	0.896	5.4	0.814	43.8	0.631	16.8	0.652	40.3	0.847	21.2	0.857	10.7
8 NCAR R1	0.881	19.1	0.602	26.5	0.177	26.3	0.671	49.0	0.682	24.9	0.695	33.7
9 20CR V2C	0.596	24.6	0.528	56.6	0.029	37.3	0.030	91.0	0.455	28.3	0.815	12.6
1 MSWEP V2.2	0.721	13.1	0.819	29.8	0.423	32.0	0.203	9.6	0.736	13.2	0.930	28.4
2 TMPA 3B42 V7	0.469	18.8	0.779	35.1	0.116	31.7	0.029	12.7	0.290	29.6	0.755	10.8
3 PERS-CDR V1R1	0.531	18.1	0.689	42.5	0.461	26.3	0.054	16.2	0.511	23.2	0.674	10.9
4 CHELSA V1.2	0.761	15.0	0.872	39.0	0.343	33.3	0.427	7.4	0.695	26.8	0.936	4.7
5 CHIRPS V2.0	0.651	21.6	0.701	53.0	0.399	33.6	0.104	9.7	0.388	24.2	0.969	3.3
6 WFDEI-CRU	0.722	12.9	0.738	51.2	0.534	30.2	0.168	11.1	0.729	15.7	0.750	29.7
7 CMAP	0.803	11.3	0.874	41.1	0.666	24.0	0.643	40.6	0.916	17.3	0.615	11.2
8 CMORPH V1.0	0.009	28.3	0.121	52.2	0.194	42.5	0.586	13.8	0.193	43.3	0.028	29.0
9 CAMSOPI	0.253	29.9	0.666	55.9	0.001	26.2	0.005	31.3	0.679	34.2	0.454	14.4

gauge-based data sets show the lowest and highest peaks during May and July respectively against June and August depicted by the reference data set in most parts except NE-Hindukush and SW-Hindukush, where highest peak is achieved during February and April respectively. The reanalysis products better reflect the wintertime precipitation but exhibit relatively large variability among them and in different regions. They record higher correlations and lower MAEs than the gauge-based and merged products particularly in higher altitude and wetter regions. Nevertheless, they consistently overestimate precipitation in drier regions of Khar Mong and SW-Hindukush throughout the year but more significantly during monsoon season. The merged products largely follow the same patterns as gauge-based products, which is understandable due to the reason that these products are derived by taking input from the gauge observations. However, the merged products exhibit larger variability as compared to gauge-based products.

They also show larger spread of error margins among themselves. CMAP and MSWEP2.2 provided higher R^2 and lower MAE as compared to their counterpart grouped data sets, except in SW-Hindukush where CHIRPS V2.0 proved to be the best in terms of both these performance metrics. The lowest MAE values in Karakoram, W-Himalaya and NE-Hindukush regions are obtained by ERA5, while CHIRPS V2.0 in SW-Hindukush and GPCC V8 in Khar Mong outperform all other data sets with the lowest MAE and highest R^2 values.

3.5 | Comparison and cross validation against adjusted streamflow

Mean annual precipitation of all gridded data sets is cross validated by the Turk-Budyko non-dimensional analysis, which is based on the factual logic that

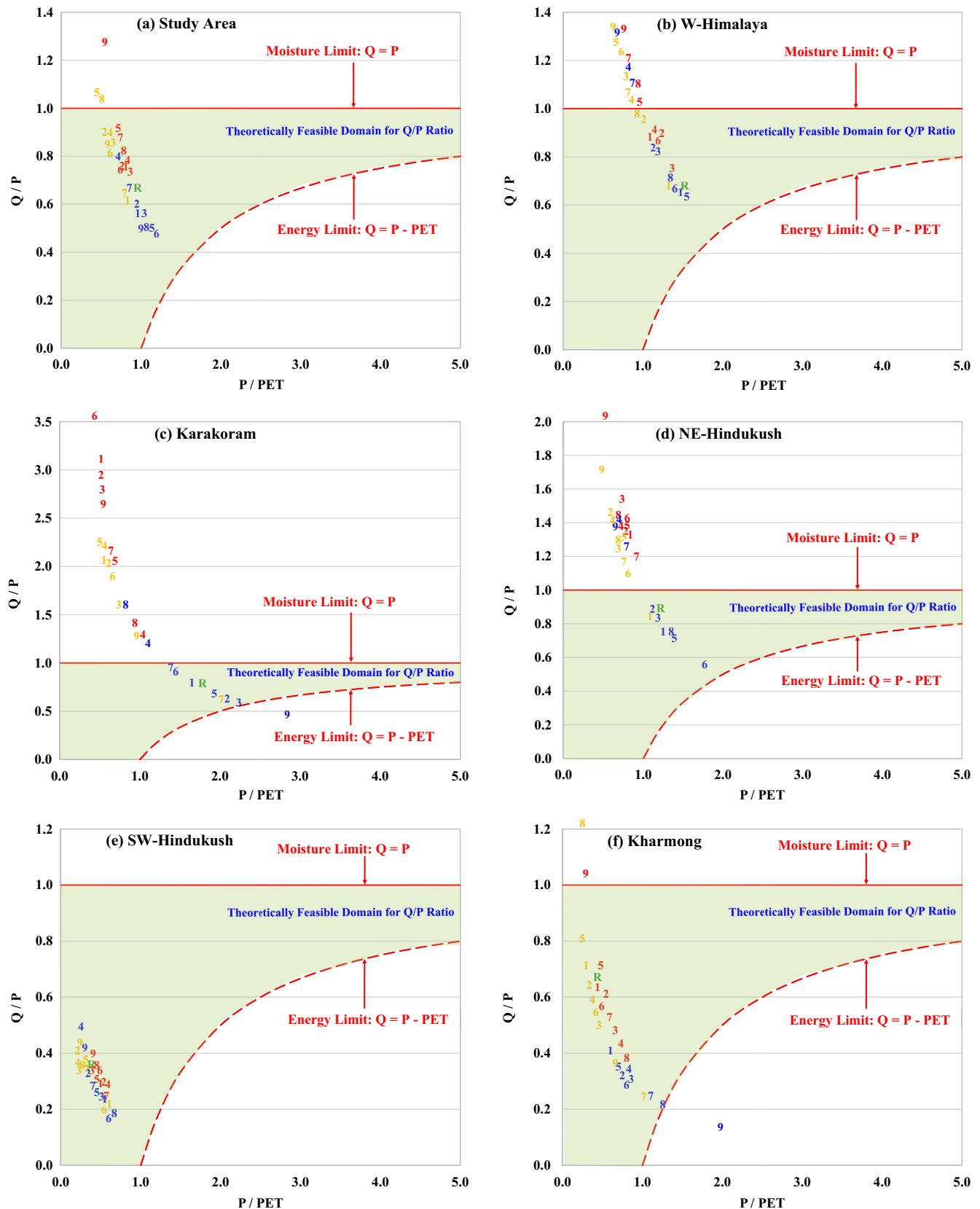


FIGURE 7 Turc-Budyko representation of runoff ratio (Q/P) and aridity indices (P/PET) for various regions of study area. Red, blue and orange coloured numbers reflect the respective names of gauge-based, reanalysis and merged data sets summarized in Table 1. The green coloured capital R represents the reference data set [Colour figure can be viewed at wileyonlinelibrary.com]

TABLE 4 Final rankings (R) and skill scores (SS) of gridded data sets derived through integration of performance metrics for study area and its various regions

R	Study Area	W-Himalaya		Karakoram		NE-Hindukush		SW-Hindukush		Kharmong		
#	Dataset	SS	Dataset	SS	Dataset	SS	Dataset	SS	Dataset	SS	Dataset	SS
1	UDEL V5.01	3.63	GPCC V8	3.77	ERA5	3.71	MSWEP V2.2	3.63	CHIRPS V2.0	4.00	GPCC V8	3.87
2	GPCC V8	3.58	UDEL V5.01	3.74	MERRA-2	3.51	ERA5	3.42	UDEL V5.01	3.76	GPCC V7	3.83
3	GPCC V7	3.55	GPCC V7	3.72	JRA-55	3.20	JRA-55	3.40	CHELSA V1.2	3.59	UDEL V5.01	3.82
4	ERA5	3.44	ERA1	3.52	CFSR	3.19	CFSR	3.27	PREC Land	3.47	CHELSA V1.2	3.53
5	APH.V1801R1	3.40	ERA5	3.45	DOE R2	3.05	MERRA-2	2.51	APH.V1101	3.27	MSWEP V2.2	3.18
6	CFSR	3.24	APH.V1801R1	3.15	ERA1	2.78	NCAR R1	1.98	TMPA 3B42 V7	3.21	APH.V1101	3.09
7	JRA-55	3.24	JRA-55	2.98	CMAP	2.53	ERA1	0.77	ERA 20C	3.21	APH.V1801R1	2.96
8	APH.V1101	3.24	MSWEP V2.2	2.85					APH.V1801R1	3.11	WFDEI-CRU	2.92
9	MSWEP V2.2	3.23	PREC Land	2.61					CFSR	3.07	CHIRPS V2.0	2.91
10	CHELSA V1.2	3.22	MERRA-2	2.49					PERS-CDR V1R1	3.04	PREC Land	2.91
11	DOE R2	3.08	CFSR	2.43					GPCP V2.3	2.99	ERA5	2.85
12	WFDEI-CRU	2.93	NCAR R1	2.04					GPCC V8	2.97	TMPA 3B42 V7	2.79
13	TMPA 3B42 V7	2.87							GPCC V7	2.96	CFSR	2.73
14	PERS-CDR V1R1	2.78							DOE R2	2.93	CMAP	2.70
15	CMAP	2.72							20CR V2C	2.90	DOE R2	2.69
16	CRU TS402	2.68							CRU TS402	2.81	PERS-CDR V1R1	2.67
17	ERA 20C	2.63							CMAP	2.75	CRU TS402	2.65
18	PREC Land	2.61							CPC Unified	2.68	ERA1	2.46
19	GPCP V2.3	2.29							MERRA-2	2.44	NCAR R1	2.43
20	MERRA-2	2.28							JRA-55	2.40	MERRA-2	2.42
21	ERA1	2.09							CAMSOP1	2.33	ERA 20C	2.40
22	NCAR R1	2.09							ERA5	2.23	JRA-55	2.40
23	CAMSOP1	1.10							MSWEP V2.2	1.53	GPCP V2.3	2.36
24	20CR V2C	0.88							WFDEI-CRU	1.37	CAMSOP1	2.16
25									CMORPH V1.0	0.83		
26									NCAR R1	0.73		
27									ERA1	0.56		

Note: Red, blue and orange colours represent gauge-based, reanalysis and merged products, respectively.

streamflow can never be greater than precipitation provided there is no contribution from the negative mass balance (glaciers) and groundwater. This study used the net streamflow adjusted for the contribution of negative mass balance determined by Dahri *et al.* (2018), so there is no question of glacier mass balance contributions. For long-term analysis, groundwater contribution to river flows is negligible in the study area. Therefore, the logic of lower streamflow than the precipitation is absolutely valid.

The Turc-Budyko diagrams presented in Figure 7 indicate that precipitation estimates by most of the gridded data sets, particularly gauge-based and merged products in higher altitude regions, are less than the corresponding streamflow, which is quite unrealistic and counterintuitive. It is also evident that most of the data sets are within the acceptable limits for the drier regions of Kharmong and SW-Hindukush. However, in higher-altitude Karakoram and NE-Hindukush regions, all gauge-based and merged products (except CMAF in Karakoram and MSWEP2.2 in NE-Hindukush) fail to

fall within the feasible domain of the Budyko curve due to their unrealistically lower precipitation than the corresponding streamflows. Similarly, for the monsoon dominated and relatively wetter region of W-Himalaya, half of the data sets show unacceptable Q/P ratios. However, such inter-regional variations offset each other when aggregated for the whole study area and except CPC-Unified, CHIRPS V2.0 and CAMSOP1 all data sets provide acceptable representation. Only ERA5, CFSR, JRA-55, MERRA-2 and ERAI are proved to be physically realistic for all regions. The other data sets fail due to underestimated precipitation in one or another region.

3.6 | Skill scores and rankings

Interestingly, a considerable inconsistency in the outcome of the applied performance metrics is noticed using the same data at the selected spatiotemporal scales. For example, AHPRODITE V1101 is found to be the best data

set in terms of MAE for the whole study area at annual scale (Figure 4c), whereas GPCC outperformed all data sets in terms of KGE score (Figure 5m). Similarly, MAE and R^2 obtained for the annual cycle of mean monthly precipitation (Table 3) suggest DOE R2 as the best data set. However, the integrated skill scores and rankings derived from the normalized values of the selected statistical indices suggest considerably different inferences than presented in the results of the individual metrics. For the whole study area, UDEL V5.01 provided the best skill score of 3.629 followed by GPCC V8 (3.579), GPCC V (3.55) and ERA5 (3.443). However, there is considerable variation in the skill scores at sub-regional scale. GPCC V8 outperforms all data sets in W-Himalaya and Khariong, ERA5 in Karakoram, MSWEP2.2 in NE-Hindukush and CHIRPS V2.0 in SW-Hindukush regions. For the combined wet and dry areas, ERA5 and UDEL V5.01 provided the highest skill scores respectively. The 20CR V2C and CMORPH V1.0 proved to be the worst performers in almost all regions. Overall, reanalysis data sets perform better in wet areas while gauge-based and merged products provided higher skill scores in dry areas. Similarly, reanalysis products outperformed other data sets in higher altitudes and gauge-based data sets provided better estimates in plain areas.

The ultimate rankings presented in Table 4 reveal that none of the gauge-based products could fall within the Budyko curve for the Karakoram and NE-Hindukush regions mainly due to their lower precipitation estimates than the corresponding streamflows. Out of merged products, only MSWEP2.2 in NE-Hindukush and CMAP in Karakoram show acceptable Q/P ratios, while majority of reanalyses retain their rankings with ERA5 performing the best. The drier regions of SW-Himalaya and Khariong are trivially affected as most of the data sets show acceptable Q/P ratios and are laid within the Budyko curve. Similarly, about half of the data sets are excluded in the monsoon dominated W-Himalaya due to higher Q/P ratios, with GPCP V8 retaining the top ranking. However, for the whole study area, the shortcomings exhibited at regional scale are offset and only CPC Unified, CHIRPS V2.0 and CMORPH V1.0 are excluded. The Turc-Budyko non-dimensional analysis is found an effective performance indicator to evaluate performance of gridded data sets. However, runoff ratio proved to be more robust indicator as compared with aridity index.

4 | DISCUSSION

This study provides a comprehensive evaluation and accuracy assessment of 27 global scale gridded precipitation products for a transboundary high-mountain Indus

basin. Widely used performance metrics are applied to evaluate and quantify the accuracy in sub-regional scale precipitation estimates of the gridded data sets with respect to a high-quality reference data set at monthly, seasonal and annual timescales. The results revealed significant errors and uncertainties in the precipitation estimates of the selected gridded precipitation data sets. The uncertainty range of the gridded data sets at annual scale ranges from -46% to $+40\%$. Most of the gridded data sets provided reasonably good patterns of seasonal precipitation distribution but displayed large differences in their precipitation magnitudes at monthly, seasonal and annual timescales in the study area. These differences are inconsistent and more pronounced at sub-regional scale (Figure 3). Overall, a large uncertainty in quantitative and spatio-temporal distribution of precipitation is evident in all gridded data sets. The results are in line with the findings of Sun *et al.* (2018), who reviewed and intercompared an ensemble of 30 global scale precipitation data sets. The most important attributions for such large differences and uncertainties in gridded precipitation products are their different structural characteristics, diverse input data and observational densities, variable quality control measures and gauge undercatch corrections, spatiotemporal resolution, and use of different interpolation schemes. The landscape heterogeneities further add to the uncertainties. Generally, precipitation differences among gridded data sets and their biases with respect to the reference data can be explained by the uncertainties in the ways and means by which these data sets are produced. The similarities in precipitation estimates of two or more data sets can often be attributed to the similar input data and methods. However, if the dissimilar data sets depict consistencies then it is very likely that such signal is present in the actual situations.

The study area is highly deficient in precipitation observations and even worse is the fact that less than one-third of the observed data are actually used by the existing gridded precipitation data sets due to strict data sharing policies of the national meteorological agencies. The situation is further worsened by the coarser spatial resolution of many gridded data sets, which limits the representation of precipitation in the high-mountain areas due to smoothing leading to underestimated peaks. Quality of the reference and gridded data sets can be improved by measuring and sharing precipitation data of the higher-altitude ranges and robust integration of mass balance data at corresponding timescales. Gauge-based data sets generally underestimate precipitation in the study area except relatively dry regions of Khariong and SW-Hindukush during monsoon season. This is obvious because higher altitude regions of Karakoram and NE-

Hindukush are highly deficient in ground-based observations. Therefore, the gauge-based data sets are derived from lower-altitude stations located in the dry valleys. The underestimated precipitation in the W-Himalaya region during winter months can be explained by lack of stations at the higher altitudes and significant under-catch of solid precipitation by the existing gauges (Dahri *et al.*, 2018). APHRODITE data set uses the largest number of station observations in the study area. Whereas, the evaluation results reveal that both of its versions significantly underestimate precipitation in most parts of the study area. GPCC and UDEL V5.01 use about half of the station observations compared to APHRODITE but provide better estimates, probably due to their efficient interpolation schemes and 5–10% correction factors applied to account for measurement errors in GPCC data (Schneider *et al.*, 2014). However, the study conducted by Dahri *et al.*, (2018) revealed that the corrections factors applied in GPCC are still on the lower side for the high-mountain Indus basin where under-catch of individual precipitation gauges varied between 2 and 182% with greater under-catches at higher altitudes and during winter months. GPCP V2.3 also applied bulk correction factors for monthly climatological conditions but its precipitation estimates are even lower than APHRODITE due to very coarse grid size, use of different data and interpolation techniques, and possibly lower correction factors. PREC Land, CRU TS4.02 and CPC-Unified use the station data shared with WMOs Global Telecommunication System (GTS), which is about half of the stations used by GPCC in the study area and employ different interpolation schemes. The gauge-based products exhibited almost similar spatial patterns but with significant differences in their precipitation magnitudes. Generally, lack of observed data at higher elevations, biased distribution of the existing stations, and measurement errors seriously limit the accuracy of gauge-based precipitation products.

Unlike gauge-based precipitation data sets, reanalysis products are significantly different from each other, because each reanalysis uses its own atmospheric model, modelling technique and data assimilation scheme (Fujiwara *et al.*, 2017; Ghodichore *et al.*, 2018). The type and number of assimilated observations also varies from one model to another. Reanalysis products mostly suffer from uncertainties in the assimilated observations, physical aspects of the reanalysis system and the model parameterizations used for weather forecast (Bosilovich *et al.*, 2008). As such, reanalysis products exhibit larger variability and wider spread of residual errors than the gauge-based and merged products. Nevertheless, winter months and higher altitude Karakoram and NE-Hindukush regions are better covered by the reanalysis products, which is in line with the findings of Beck

et al. (2019) and general characteristics of reanalysis providing better estimates for the frontal system precipitation during cooler seasons. The largest errors are observed during monsoon season, which is probably due to the convective nature of monsoon precipitation and high uncertainties in deep convection parameterization schemes applied in the reanalysis models. They also better follow the peaks. Annual cycle of area-weighted mean monthly precipitation is also better reflected in wet areas. Yet, precipitation in dry areas is largely overestimated by reanalysis products.

The development of merged precipitation products aims to exploit the complementary nature and comparative advantages of ground-based observations, reanalysis and/or satellite data leading to higher quality end products. However, the merged products inherit the limitations of their source data and are also affected by the uncertainties in the merging algorithms. Most of the gauge-observations used to calibrate satellite products and develop merged products are extracted from GTS network with poor spatial coverage in the HKH region (Yatagai *et al.*, 2012). This could explain the underestimated precipitation by the resultant products at higher altitudes. Since, the merged products take inputs from the ground observations, they are closer to the gauge-based products. Yet, they exhibit a larger variability and error spreads among themselves due to differences in other data sources. Surprisingly, the performance of merged products in most parts of the study area is worse than many gauge-based and reanalysis products. This can partly be attributed to use of different and/or less observations. However, the major reason might be the problem in merging techniques, which are unable to preserve the comparative advantages of the gauge, reanalysis and satellite data. The quality of any merged products should be better than its parent input data sets, which might be true in data rich regions, but it is not the case in a data scarce high-altitude Indus basin.

Generally, errors or uncertainties in terms of over- and/or under-estimation of precipitation are ascertained in relative terms against a reference data set. However, if the reference data differ in their precipitation patterns and magnitudes, the performance of the gridded data sets may change accordingly. The reference data set used in this study is unique and has never been used before for evaluation purpose. Therefore, the patterns and magnitudes of errors in precipitation estimates of the gridded data sets deduced in this study are also unique and may not be compared precisely with earlier studies, which used different benchmarks. Although, the quality of precipitation distributions in the reference data set was found consistent with the corresponding river inflows

(Dahri *et al.*, 2018), the authors also described the associated uncertainties, minimization of which will result in higher quality reference data set. These uncertainties are mainly attributed to amount, quality and distribution of precipitation observations; uncertainties in error-adjustment regression models due to their imprecision; and uncertainties in spatial interpolation of the point observations. It is also pertinent to note that the reference data set used in this study includes monthly means of the error-adjusted precipitation observations for the period of 1999–2011, the best evaluation results can be achieved at similar temporal resolution and scale. The data beyond this temporal scale are assumed to follow similar trends in the biases and are liable to some degree of uncertainty. It would be advisable to extend the evaluation using long term daily and monthly time series once the high-quality reference data set at such temporal scales is made available. The evaluation at daily timestep would be useful to select the better data sets for assessing precipitation extremes and subsequent droughts or floods. Moreover, the Turc-Budyko non-dimensional analysis largely depends on the Q/P ratio, which is subject to uncertainties in the quality of river flows data. Study conducted by IRSA (2015) indicated an overall uncertainty of 3–8% in the river/canal discharge measurement protocols adopted in the Indus river system. Moreover, any improvement in the estimates of glacier mass balance and glacier area used by the reference data set for adjustment of river inflows may slightly affect the cross-validation of the reference data set but would have insignificant effect on the end results of this study.

The global/continental scale precipitation products are developed from different sources using the techniques, which are more suitable at larger spatial scales but are relatively inefficient at smaller (country or catchment) scale. While the underlying efforts to develop merged data sets have been focusing on merging/combining data from different sources, another alternative may be to first develop regional/national/basin scale data sets using optimum data and techniques and then merge/mosaic these products to form a high-quality product at global scale.

5 | CONCLUSIONS

This study highlighted and corroborated the underlying issues and uncertainties associated with a wide range of gridded precipitation products in the high-mountain Indus basin. The results clearly indicate that all gridded data sets evaluated in this study contain significant errors in their precipitation estimates and cannot be used directly without careful bias correction. The following major conclusions are drawn.

1. All gridded data sets tend to underestimate precipitation in wet areas and overestimate precipitation in dry areas, implying considerable implications for hydrological extremes of floods and droughts. GPCC V8, ERA5 and MSWEP2.2 provided better estimates than their counter-groups of gauge-based, reanalysis and merged data sets. ERA5 and UDEL V5.01 provided the highest skill scores for wet and dry areas, respectively.
2. None of the data set is equally best for all sub-regions of the study area. A particular data set performing very well in one sub-region is found worse in the other sub-region. Nevertheless, ERA5 is found most acceptable for all sub-regions. This study therefore would provide useful guidance for selection and use of the best data set for a particular sub-region or sub-basin for hydrometeorological assessments.
3. Due to large uncertainties in the gauge-based precipitation products in the higher-altitude Karakoram and NE-Hindukush regions, a general perception is that precipitation from uncalibrated reanalysis products might be closer to the actual precipitation. This study, however, revealed that reanalysis data sets provide relatively better estimates for the higher-altitude areas where observations are generally scarce. However, not all reanalysis products can serve the purpose due to large differences in their precipitation patterns and magnitudes. Therefore, a careful selection is deemed essential.
4. Relatively poor performance of the merged data sets in the study region highlights their weaknesses and inability to accurately estimate precipitation and underlines the need to develop more advanced and accurate merging techniques, which can preserve the comparative advantages of their input data sets and are equally accurate at catchment scales.
5. In Turc-Budyko non-dimensional analysis, runoff ratio proved to be the dominant/decisive indicator to single out the data sets that underestimate precipitation, while aridity index appears to be a softer indicator to distinguish the overestimating data sets, as none of the evaluated data set could be rejected or chosen on the basis of aridity index.

ACKNOWLEDGEMENTS

This research work is supported by the Netherlands Fellowship Program and partially carried out under the Himalayan Adaptation, Water and Resilience (HI-AWARE) consortium. The views expressed in this work do not necessarily represent those of the supporting organizations. Deepest gratitude is expressed to the institutions and the teams responsible for the development and distribution

of the gridded precipitation data sets used in this study. The authors declare that there is no conflict of interest.

ORCID

Zakir Hussain Dahri  <https://orcid.org/0000-0002-0922-951X>

Muhammad Saleem Pomee  <https://orcid.org/0000-0003-1496-4663>

REFERENCES

- Adler, R.F., Sapiiano, M.R.P., Huffman, G.J., Wang, J.-J., Gu, G., Bolvin, D., Chiu, L., Schneider, U., Becker, A., Nelkin, E., Xie, P., Ferraro, R. and Shin, D.-B. (2018) The global precipitation climatology project (GPCP) monthly analysis (new version 2.3) and a review of 2017 global precipitation. *Atmosphere*, 9, 138. <https://doi.org/10.3390/atmos9040138>.
- Aghakouchak, A., Mehran, A., Norouzi, H. and Behrangi, A. (2012) Systematic and random error components in satellite precipitation data sets. *Geophysical Research Letters*, 39(9), 3, L09406–6. <https://doi.org/10.1029/2012GL051592>.
- Ahmed, K., Shahid, S., Wang, X., Nawaz, N. and Najeebullah, K. (2019) Evaluation of gridded precipitation datasets over arid regions of Pakistan. *Water*, 11, 210.
- Ali, G., Rasul, G., Mahmood, T., Zaman, Q. and Cheema, S.B. (2012) Validation of APHRODITE precipitation data for humid and sub humid regions of Pakistan. *Pakistan Journal of Meteorology*, 9(17), 57–69.
- Andermann, C., Bonnet, S. and Gloaguen, R. (2011) Evaluation of precipitation data sets along the Himalayan front, geochemistry, *Geophys. Geosystems*, 12(7), 1–16. <https://doi.org/10.1029/2011GC003513>.
- Anders, A.M., Roe, G.H., Hallet, B., Montgomery, D.R., Finnegan, N. J. and Putkonen, J. (2006) Spatial patterns of precipitation and topography in the Himalaya. In: Willett, S.D., Hovius, N., Brandon, M.T. and Fisher, D. (Eds.) *Tectonics, Climate, and Landscape Evolution*. 3300 Penrose Place, P.O. Box 9140, Boulder, Colorado 80301-9140, USA: Geological Society of America Special Paper 398, pp. 39–53. [https://doi.org/10.1130/2006.2398\(03\)](https://doi.org/10.1130/2006.2398(03)).
- Andréassian, V. and Perrin, C. (2012) On the ambiguous interpretation of the Turc-Budyko nondimensional graph. *Water Resources Research*, 48, W10601. <https://doi.org/10.1029/2012WR012532>.
- Anjum, M.N., Ding, Y., Shangguan, D., Ahmad, I., Ijaz, M.W., Farid, H.U., Yagoub, Y.E., Zaman, M. and Adnan, M. (2018) Performance evaluation of latest integrated multi-satellite retrievals for global precipitation measurement (IMERG) over the northern highlands of Pakistan. *Atmospheric Research*, 205, 134–146 <https://doi.org/10.1016/j.atmosres.2018.02.010>.
- Arendt, A., Bliss, A., Bolch, T., Cogley, J. G., Gardner, A. S., Hagen, J.-O., Hock, R., Huss, M., Kaser, G., Kienholz, C., Pfeffer, W.T., Moholdt, G., Paul, F., Radić, V., Andreassen, L., Bajracharya, S., Barrand, N.E., Beedle, M., Berthier, E., Bhambri, R., Brown, I., Burgess, E., Burgess, D., Cawkwell, F., Chinn, T., Copland, L., Davies, B., De Angelis, H., Dolgova, E., Earl, L., Filbert, K., Forester, R., Fountain, A.G., Frey, H., Giffen, B., Glasser, N., Guo, W.Q., Gurney, S., Hagg, W., Hall, D., Haritashya, U.K., Hartmann, G., Helm, C., Herreid, S., Howat, I., Kapustin, G., Khromova, T., König, M., Kohler, J., Kriegel, D., Kutuzov, S., Lavrentiev, I., LeBris, R., Liu, S.Y., Lund, J., Manley, W., Marti, R., Mayer, C., Miles, E.S., Li, X., Menounos, B., Mercer, A., Mölg, N., Mool, P., Nosenko, G., Negrete, A., Nuimura, T., Nuth, C., Pettersson, R., Racoviteanu, A., Ranzani, R., Rastner, P., Rau, F., Raup, B., Rich, J., Rott, H., Sakai, A., Schneider, C., Seliverstov, Y., Sharp, M., Sigurdsson, O., Stokes, C., Way, R.G., Wheate, R., Winsvold, S., Wolken, G. and Wyatt, F. (2015) Randolph glacier inventory—a dataset of global glacier outlines: version 5.0 (GLIMS Technical Report).
- Ashouri, H., Hsu, K.-L., Sorooshian, S., Braithwaite, D.K., Knapp, K.R., Cecil, L.D. and Prat, O.P. (2015) PERSIANN-CDR: daily precipitation climate data record from multi-satellite observations for hydrological and climate studies. *Bulletin of the American Meteorological Society*, 96(1), 69–83. <https://doi.org/10.1175/BAMS-D-13-00068.1>.
- Beck, H.E., van Dijk, A.I.J.M., Levizzani, V., Schellekens, J., Miralles, D.G., Martens, B. and de Roo, A. (2017) MSWEP: 3-hourly 0.25° global gridded precipitation (1979–2015) by merging gauge, satellite, and reanalysis data. *Hydrology and Earth System Sciences*, 21, 589–615 <https://doi.org/10.5194/hess-21-589-2017>.
- Beck, H.E., Wood, E.F., Pan, M., Fisher, C.K., Miralles, D.M., van Dijk, A.I.J.M., McVicar, T.R. and Adler, R.F. (2019) MSWEP V2 global 3-hourly 0.1° precipitation: methodology and quantitative assessment. *Bulletin of the American Meteorological Society*, 100(3), 473–500. <https://doi.org/10.1175/BAMS-D-17-0138.1>.
- Boers, N., Bookhagen, B., Marwan, N. and Kurths, J. (2016) Spatiotemporal characteristics and synchronization of extreme rainfall in South America with focus on the Andes mountain range. *Climate Dynamics*, 46, 601–617.
- Böhner, J. (2006) *General Climatic Controls and Topoclimatic Variations in Central and High Asia*, Vol. 35. Oslo: Boreas, pp. 279–295. <https://doi.org/10.1080/03009480500456073>.
- Bolch, T., Kulkarni, A., Kääb, A., Huggel, C., Paul, F., Cogley, J.G., Frey, H., Kargel, J.S., Fujita, K., Scheel, M., Bajracharya, S. and Stoffel, M. (2012) The state and fate of Himalayan glaciers. *Science*, 336, 310–314 <https://doi.org/10.1126/science.1215828>.
- Bosilovich, M.G., Chen, J., Robertson, F.R. and Adler, R.F. (2008) Evaluation of global precipitation in reanalysis. *Journal of Applied Meteorology and Climatology*, 47, 2279–2299. <https://doi.org/10.1175/2008JAMC1921.1>.
- Budyko, M.I. (1974) *Climate and Life*. Orlando, FL: Academic Press, p. 508.
- Chai, T. and Draxler, R.R. (2014) Root mean square error (RMSE) or mean absolute error (MAE)? - arguments against avoiding RMSE in the literature. *Geoscientific Model Development*, 7, 1247–1250.
- Chen, M., Shi, W., Xie, P., Silva, V.B.S., Kousky, V.E., Higgins, R.W. and Janowiak, J.E. (2008) Assessing objective techniques for gauge-based analyses of global daily precipitation. *Journal of Geophysical Research*, 113, D04110 <https://doi.org/10.1029/2007JD009132>.
- Chen, M.P., Xie, P., Janowiak, J.E. and Arkin, P.A. (2002) Global land precipitation: a 50-yr monthly analysis based on gauge observations. *Journal of Hydrometeorology*, 3, 249–266.

- Ciabatta, L., Massari, C., Brocca, L., Gruber, A., Reimer, C., Hahn, S., Paulik, C., Dorigo, W., Kidd, R. and Wagner, W. (2018) SM2RAIN-CCI: 20A new global long-term rainfall data set derived from ESA CCI soil moisture. *Earth System Science Data*, 10, 267–280.
- Compo, G.P., Whitaker, J.S., Sardeshmukh, P.D., Matsui, N., Allan, R.J., Yin, X., Gleason, B.E., Vose, R.S., Rutledge, G., Bessemoulin, P., Brönnimann, S., Brunet, M., Crouthamel, R.I., Grant, A.N., Groisman, P.Y., Jones, P.D., Kruk, M.C., Kruger, A.C., Marshall, G.J., Maugeri, M., Mok, H.Y., Nordli, Ø., Ross, T.F., Trigo, R.M., Wang, X.L., Woodruff, S.D. and Worley, S.J. (2011) The twentieth century reanalysis project. *Quarterly Journal of the Royal Meteorological Society*, 137, 1–28.
- Coron, L., Andréassian, V., Perrin, C. and Le Moine, N. (2015) Graphical tools based on Turc-Budyko plots to detect changes in catchment behaviour. *Hydrological Sciences Journal*, 60(7–8), 1394–1407. <https://doi.org/10.1080/02626667.2014.964245>.
- Dahri, Z.H., Ludwig, F., Moors, E., Ahmad, B., Khan, A. and Kabat, P. (2016) An appraisal of precipitation distribution in the high-altitude catchments of the Indus basin. *Science of the Total Environment*, 548–549, 289–306.
- Dahri, Z.H., Moors, E., Ludwig, F., Ahmad, S., Khan, A., Ali, I. and Kabat, P. (2018) Adjustment of measurement errors to reconcile precipitation distribution in the high-altitude Indus basin. *International Journal of Climatology*, 2018, 1–19 <https://doi.org/10.1002/joc.5539>.
- de Kok, R.J., Tuinenburg, O.A., Bonekamp, P.N.J. and Immerzeel, W.W. (2018) Irrigation as a potential driver for anomalous glacier behavior in high mountain asia. *Geophysical Research Letters*, 45(4), 2047–2054. <https://doi.org/10.1002/2017GL076158>.
- De Souza, K., Kituyi, E., Leone, M., Harvey, B., Murali, K.S. and Ford, J. (2015) Vulnerability to climate change in three hot spots in Africa and Asia: key issues for policy-relevant adaptation and resilience-building research. *Regional Environmental Change*, 15(5), 747–753. <https://doi.org/10.1007/s10113-015-0755-8>.
- Dee, D.P., Uppala, S., Simmons, A., Berrisford, P., Poli, P., Kobayashi, S., Andrae, U., Balmaseda, M., Balsamo, G., Bauer, d.P., Bechtold, P., Beljaars, A.C.M., van de Berg, L., Bidlot, J., Bormann, N., Delsol, C., Dragani, R., Fuentes, M., Geer, A.J., Haimberger, L., Healy, S.B., Hersbach, H., Hólm, E. V., Isaksen, I., Kållberg, P., Köhler, M., Matricardi, M., McNally, A.P., Monge-Sanz, B.M., Morcrette, J.J., Park, B.K., Peubey, C., de Rosnay, P., Tavolato, C., Thépaut, J.N. and Vitart, F. (2011) The ERA-interim reanalysis: configuration and performance of the data assimilation system. *Quarterly Journal of the Royal Meteorological Society*, 137, 553–597.
- Ding, Y.H. and Chan, J.C.L. (2005) The east Asian summer monsoon: an overview. *Meteorology and Atmospheric Physics*, 89, 117–142 <https://doi.org/10.1007/s00703-005-0125-z>.
- Ebert, E.E., Janowiak, J.E. and Kidd, C. (2007) Comparison of near-real-time precipitation estimates from satellite observations and numerical models. *Bulletin of the American Meteorological Society*, 88(1), 47–64.
- Filippi, L., Palazzi, E., von Hardenberg, J. and Provenzale, A. (2014) Multidecadal variations in the relationship between the NAO and winter precipitation in the Hindu-Kush Karakoram. *Journal of Climate*, 27(20), 7890–7902. <https://doi.org/10.1175/JCLI-D-14-00286.1>.
- Fowler, H.J. and Archer, D.R. (2006) Conflicting signals of climatic change in the upper Indus Basin. *Journal of Climate* 2006, 19, 4276–4293. <https://doi.org/10.1175/JCLI3860.1>.
- Fujiwara, M., Wright, J.S., Manney, G.L., Gray, L.J., Anstey, J., Birner, T., Davis, S., Gerber, E.P., Harvey, V.L., Hegglin, M.I., Homeyer, C.R., Knox, J.A., Krüger, K., Lambert, A., Long, C.S., Martineau, P., Molod, A., Monge-Sanz, B.M., Santee, M.L., Tegtmeier, S., Chabrillat, S., Tan, D.G.H., Jackson, D.R., Polavarapu, S., Compo, G.P., Dragani, R., Ebisuzaki, W., Harada, Y., Kobayashi, C., McCarty, W., Onogi, K., Pawson, S., Simmons, A., Wargan, K., Whitaker, J.S. and Zou, C.-Z. (2017) Introduction to the SPARC reanalysis Intercomparison project (S-RIP) and overview of the reanalysis systems. *Atmospheric Chemistry and Physics*, 17, 1417–1452. <https://doi.org/10.5194/acp-17-1417-2017>.
- Funk, C., Peterson, P., Landsfeld, M., Pedreros, D., Verdin, J., Shukla, S., Husak, G., Rowland, J., Harrison, L., Hoell, A. and Michaelsen, J. (2015b) The climate hazards infrared precipitation with stations – a new environmental record for monitoring extremes. *Scientific Data*, 2, 150066. <https://doi.org/10.1038/sdata.2015.66>.
- Funk, C., Verdin, A., Michaelsen, J., Peterson, P., Pedreros, D., and Husak, G. (2015a) A global satellite-assisted precipitation climatology. *Earth System Science Data*, 7(2), 275–287. <http://dx.doi.org/10.5194/essd-7-275-2015>.
- Gampe, D. and Ludwig, R. (2017) Evaluation of gridded precipitation data products for hydrological applications in complex topography. *Hydrology*, 4, 53. <https://doi.org/10.3390/hydrology4040053>.
- Gebremichael, M. (2010) Framework for satellite rainfall product evaluation. *Geophysical Monograph Series, American Geophysical Union*, 191, 265–275. <https://doi.org/10.1029/2010GM000974>.
- Gelaro, R., McCarty, W., Suárez, M.J., Todling, R., Molod, A., Takacs, L., Randles, C.A., Darmenov, A., Bosilovich, M.G., Reichle, R., Wargan, K., Coy, L., Cullather, R., Draper, C., Akella, S., Buchard, V., Conaty, A., da Silva, A.M., Gu, W., Kim, G.K., Koster, R., Lucchesi, R., Merkova, D., Nielsen, J.E., Partyka, G., Pawson, S., Putman, W., Rienecker, M., Schubert, S.D., Sienkiewicz, M. and Zhao, B. (2017) The modern-era retrospective analysis for research and applications, version 2 (MERRA-2). *Journal of Climate*, 30, 5419–5454.
- Ghodichore, N., Vinnarasi, R., Dhanya, C.T. and Roy, S.B. (2018) Reliability of reanalysis products in simulating precipitation and temperature characteristics over India. *Journal of Earth System Science*, 127, 115. <https://doi.org/10.1007/s12040-018-1024-2>.
- Ghulami, M., Babel, M.S. and Shrestha, M.S. (2017) Evaluation of gridded precipitation datasets for the Kabul Basin, Afghanistan. *International Journal of Remote Sensing*, 38(11), 3317–3332.
- Goodison, B.E., Louie, P.Y.T. and Yang, D. (1998) *WMO Solid Precipitation Measurement Intercomparison, Instruments and Observing Methods (Final Report No. 67, WMO/TD-No. 872)*. Geneva, Switzerland: World Meteorological Organization.
- Gupta, H.V., Kling, H., Yilmaz, K.K. and Martinez-Baquero, G.F. (2009) Decomposition of the mean squared error & NSE performance criteria: implications for improving hydrological

- modelling. *Journal of Hydrology*, 377, 80–91. <https://doi.org/10.1016/j.jhydrol.2009.08.003>.
- Harding, R.J., Blyth, E.M., Tuinenburg, O.A. and Wiltshire, A. (2013) Land atmosphere feedbacks and their role in the water resources of the Ganges basin. *Science of the Total Environment*, 468–469, S85–S92. <https://doi.org/10.1016/j.scitotenv.2013.03.016>.
- Harris, I.C. and Jones, P.D. (2019): CRU TS4.02: Climatic Research Unit (CRU) Time-Series (TS) version 4.02 of high-resolution gridded data of month-by-month variation in climate (Jan. 1901– Dec. 2017). Centre for Environmental Data Analysis, April 1, 2019, University of East Anglia Climatic Research Unit. doi:<https://doi.org/10.5285/b2f81914257c4188b181a4d8b0a46bff>.
- Henn, B., Newman, A.J., Livneh, B., Daly, C. and Lundquist, J.D. (2018) An assessment of differences in gridded precipitation datasets in complex terrain. *Journal of Hydrology*, 556, 1205–1219. <https://doi.org/10.1016/j.jhydrol.2017.03.008>.
- Hersbach, H., de Rosnay, P., Bell, B., Schepers, D., Simmons, A., Soci, C., Abdalla, S., Alonso-Balmaseda, M., Balsamo, G., Bechtold, P., 10 Berrisford, P., Bidlot, J.-R., de Boissésón, E., Bonavita, M., Browne, P., Buizza, R., Dahlgren, P., Dee, D., Dragani, R., Diamantakis, M., Flemming, J., Forbes, R., Geer, A., Haiden, T., Hólm, E., Haimberger, L., Hogan, R., Horányi, A., Janiskova, M., Laloyaux, P., Lopez, P., Munoz-Sabater, J., Peubey, C., Radu, R., Richardson, D., Thépaut, J.-N., Vitart, F., Yang, X., Zsótér, E., and Zuo, H. (2018) Operational global reanalysis: progress, future directions and synergies with NWP, ERA-report, Serie 27, <https://doi.org/10.21957/tkic6g3wm>,
- Hodges, K. (2006) Climate and the evolution of mountains. *Scientific American*, 295(2), 72–79.
- Huffman, G.J., Bolvin, D.T. and Nelkin, E.J. (2018) Integrated Multi-satellite Retrievals for GPM (IMERG). Technical Documentation, Tech. rep., NASA/GSFC, Greenbelt, MD 20771, USA.
- Huffman, G.J., Bolvin, D.T., Nelkin, E.J., Wolff, D.B., Adler, R.F., Gu, G., Hong, Y., Bowman, K.P. and Stocker, E.F. (2007) The TRMM multisatellite precipitation analysis (TMPA): quasi-global, multiyear, combined-sensor precipitation estimates at fine scales. *Journal of Hydrometeorology*, 8(1), 38–55.
- Hussain, S., Song, X., Ren, G., Hussain, I., Han, G. and Zaman, M. H. (2017) Evaluation of gridded precipitation data in the Hindu Kush-Karakoram-Himalaya mountainous area. *Hydrological Sciences Journal*. 62(14), 2393–2405. <https://doi.org/10.1080/02626667.2017.1384548>.
- Immerzeel, W.W., Wanders, N., Lutz, A.F., Shea, J.M. and Bierkens, M.F.P. (2015a) Reconciling high-altitude precipitation in the upper Indus basin with glacier mass balances and runoff. *Hydrology and Earth System Sciences*, 19, 4673–4687. <https://doi.org/10.5194/hess-19-4673-2015>.
- Immerzeel, W.W., Wanders, N., Lutz, A.F., Shea, J.M. and Bierkens, M.F.P. (2015b) Reconciling high altitude precipitation in the upper Indus Basin with glacier mass balances and runoff. *Hydrology and Earth System Sciences*, 19, 4673–4687. <https://doi.org/10.5194/hessd-12-4755-2015>.
- Iqbal, M., Dahri, Z., Querner, E., Khan, A. and Hofstra, N. (2018) Impact of climate change on flood frequency and intensity in the Kabul River basin. *Geosciences*, 8(4), 114. <https://doi.org/10.3390/geosciences8040114>.
- IRSA (2015), Improvement of Water Resources Management of Indus Basin to Enhance the Capacity of Indus River System Authority, Volume 1, Final Report, Indus River System Authority (IRSA).
- Janowiak, J.E. and Xie, P. (1999) CAMS-OPI: a global satellite-rain gauge merged product for real-time precipitation monitoring applications. *Journal of Climate*, 12, 3335–3342.
- Joseph, R., Smith, T.M., Sapiano, M.R.P. and Ferraro, R.R. (2009) A new high-resolution satellite-derived precipitation dataset for climate studies. *Journal of Hydrometeorology*, 10, 935–952.
- Kääb, A., Berthier, E., Christopher, N., Gardelle, J. and Arnaud, Y. (2012) Contrasting patterns of early twenty-first-century glacier mass change in the Himalayas. *Nature*, 488(7412), 495–498.
- Kalnay, E., Kanamitsu, M., Kistler, R., Collins, W., Deaven, D., Gandin, L., Iredell, M., Saha, S., White, G., Woollen, J., Zhu, Y., Leetmaa, A., Reynolds, R., Chelliah, M., Ebisuzaki, W., Higgins, W., Janowiak, J., Mo, K.C., Ropelewski, C., Wang, J., Jenne, R. and Joseph, D. (1996) The NCEP/NCAR 40-year reanalysis project. *Bulletin of the American Meteorological Society*, 77(3), 437–471. [https://doi.org/10.1175/1520-0477\(1996\)077<0437:TNYRP>2.0.CO;2](https://doi.org/10.1175/1520-0477(1996)077<0437:TNYRP>2.0.CO;2).
- Kanamitsu, M., Ebisuzaki, W., Woollen, J., Yang, S.-K., Hnilo, J., Fiorino, M. and Potter, G. (2002) Ncep-doe amip-ii reanalysis (r-2). *Bulletin of the American Meteorological Society*, 83, 1631–1644.
- Karger, D.N., Conrad, O., Böhner, J., Kawohl, T., Kreft, H., Soria-Auza, R.W., Zimmermann, N.E., Linder, H.P. and Kessler, M. (2017) Climatologies at high resolution for the earth land surface areas. *Scientific Data*, 4, 170122. <https://doi.org/10.1038/sdata.2017.122>.
- Khan, A.J., Koch, M. and Chinchillaet, K.M. (2018) Evaluation of gridded multi-satellite precipitation estimation (TRMM-3B42-V7) performance in the upper Indus Basin (UIB). *Climate* 2018, 6, 76. <https://doi.org/10.3390/cli6030076>.
- Kling, H., Fuchs, M. and Paulin, M. (2012) Runoff conditions in the upper Danube basin under an ensemble of climate change scenarios. *Journal of Hydrology*, 424–425, 264–277. <https://doi.org/10.1016/j.jhydrol.2012.01.001>.
- Kobayashi, S., Ota, Y., Harada, Y., Ebata, A., Moriya, M., Onoda, H., Onogi, K., Kamahori, H., Kobayashi, C., Endo, H., Miyaoka, K. and Takahashi, K. (2015) The JRA-55 reanalysis: general specifications and basic characteristics. *Journal of the Meteorological Society of Japan. Ser. I*, 93, 5–48 <https://doi.org/10.2151/jmsj.2015-001>.
- Krakauer, N.Y., Lakhankar, T. and Dars, G.H. (2019) Precipitation trends over the Indus basin. *Climate*, 7(10), 116–135. <https://doi.org/10.3390/cli7100116>.
- Krishnan, R., Shrestha, A.B., Ren, G., Rajbhandari, R., Saeed, S., Sanjay, J., Syed, M.A., Vellore, R., Xu, Y., You, Q. and Ren, Y. (2019) Unravelling climate change in the Hindu Kush Himalaya: rapid warming in the mountains and increasing extremes. In: Wester, P., Mishra, A., Mukherji, A. and Shrestha, A. (Eds.) *The Hindu Kush Himalaya Assessment*. Cham: Springer, pp. 57–97.
- Legates, D.R. and Willmott, C.J. (1990) Mean seasonal and spatial variability in gauge-corrected global precipitation. *International Journal of Climatology*, 10, 111–127.
- Lundquist, J.D., Minder, J.R., Neiman, P.J. and Sukovich, E. (2010) Relationships between barrier jet heights, orographic

- precipitation gradients and streamflow in the northern Sierra Nevada. *Journal of Hydrometeorology*, 11, 1141–1156.
- Lutz, A.F., Immerzeel, W.W., Kraaijenbrink, P.D.A., Shrestha, A.B. and Bierkens, M.F.P. (2016) Climate change impacts on the upper Indus hydrology: sources, shifts and extremes. *PLoS One*, 11(11), e0165630. <https://doi.org/10.1371/journal.pone.0165630>.
- Lutz, A.F., Immerzeel, W.W., Shrestha, A.B. and Bierkens, M.F.P. (2014) Consistent increase in high Asia's runoff due to increasing glacier melt and precipitation. *Nature Climate Change*, 4(7), 587–592. <https://doi.org/10.1038/nclimate2237>.
- Lutz, A.F., Maat, H.W., Wijngaard, R.R., Biemans, H., Syed, A., Shrestha, A.B., Wester, P. and Immerzeel, W.W. (2018) South Asian river basins in a 1.5°C warmer world. *Regional Environmental Change*, 19(3), 833–847. <https://doi.org/10.1007/s10113-018-1433-4>.
- Maggioni, V., Sapiano, M.R.P. and Adler, R.F. (2016) Estimating uncertainties in high-resolution satellite precipitation products: systematic or random error? *Journal of Hydrometeorology*, 17 (4), 1119–1129 <https://doi.org/10.1175/jhm-d-15-0094.1>.
- Matsuura, K. and Willmott, C. (2018) Terrestrial Precipitation: 1900–2014, Gridded Monthly Time Series (1900–2014), V5.01, University of Delaware. Available online: https://www.esrl.noaa.gov/psd/data/gridded/data/UDel_AirT_Precip.html#detail, documentation: http://climate.geog.udel.edu/~climate/html_pages/Global2017/README.GlobalTsP2017.html
- Mayer, C., Lambrecht, A., Oerter, H., Schwikowski, M., Vuillermoz, E., Frank, N., and Diolaiuti, G. (2014) Accumulation studies at a high elevation glacier site in central karakoram. *Advances in Meteorology*, 2014, 1–12. <http://dx.doi.org/10.1155/2014/215162>.
- Pal, I., Robertson, A.W., Lall, U. and Cane, M.A. (2014) Modeling winter rainfall in Northwest India using a hidden Markov model: understanding occurrence of different states and their dynamical connections. *Climate Dynamics*, 44(3), 1003–1015. <https://doi.org/10.1007/s00382-014-2178-5>.
- Palazzi, E., Hardenberg, J. and Provenza, A. (2013) Precipitation in the Hindu-Kush Karakoram Himalaya: observations and future scenarios. *Journal of Geophysical Research-Atmospheres*, 118, 85–100 <https://doi.org/10.1029/2012JD018697>.
- Pang, H., Hou, S., Kaspari, S. and Mayewski, P.A. (2014) Influence of regional precipitation patterns on stable isotopes in ice cores from the Central Himalayas. *The Cryosphere*, 8, 289–301 <https://doi.org/10.5194/tc-8-289-2014>.
- Peña-Arancibia, J.L., van Dijk, A.I.J.M., Renzullo, L.J. and Mulligan, M. (2013) Evaluation of precipitation estimation accuracy in reanalysis, satellite products, and an ensemble method for regions in Australia and Sout and East Asia. *Journal of Hydrometeorology*, 14, 1323–1333. <https://doi.org/10.1175/JHM-D-12-0132.1>.
- Prein, A.F. and Gobiet, A. (2017) Impacts of uncertainties in European gridded precipitation observations on regional climate analysis. *International Journal of Climatology*, 37, 305–327. <https://doi.org/10.1002/joc.4706>.
- Putkonen, J. (2004) Continuous snow and rain data at 500 to 4400 m altitude near Annapurna, Nepal, 1999–2001. *Arctic, Antarctic, and Alpine Research*, 36, 244–248. [https://doi.org/10.1657/1523-0430\(2004\)036\[0244:CSARDA\]2.0.CO;2](https://doi.org/10.1657/1523-0430(2004)036[0244:CSARDA]2.0.CO;2).
- Rasmussen, R., Baker, B., Kochendorfer, J., Meyers, T., Landolt, S., Fischer, A.P., Black, J., Theriault, J.M., Kucera, P., Gochis, D., Smith, C., Nitu, R., Hall, M., Ikeda, K. and Gutmann, E. (2012) How well are we measuring snow: the NOAA/FAA/NCAR winter precipitation test bed. *Bulletin of the American Meteorological Society*, 93(6), 811–829. <https://doi.org/10.1175/BAMS-D-11-00052.1>.
- Reggiani, P. and Rientjes, T.H.M. (2015) A reflection on the long-term water balance of the upper Indus basin. *Hydrology Research*, 46, 446–462 <https://doi.org/10.2166/nh.2014.060>.
- Ruane, A.C. and Roads, J.O. (2007) 6-hour to 1-year variance of five global precipitation sets. *Earth Interactions*, 11. [Available online at <http://EarthInteractions.org>].
- Saha, S., Moorthi, S., Pan, H.-L., Wu, X., Wang, J., Nadiga, S., Tripp, P., Kistler, R., Woollen, J., Behringer, D., Liu, H., Stokes, D., Grumbine, R., Gayno, G., Wang, J., Hou, Y.-T., Chuang, H.Y., Juang, H.-M.H., Sela, J., Iredell, M., Treadon, R., Kleist, D., Van Delst, P., Keyser, D., Derber, J., Ek, M., Meng, J., Wei, H., Yang, R., Lord, S., Van Den Dool, H., Kumar, A., Wang, W., Long, C., Chelliah, M., Xue, Y., Huang, B., Schemm, J.-K., Ebisuzaki, W., Lin, R., Xie, P., Chen, M., Zhou, S., Higgins, W., Zou, C.-Z., Liu, Q., Chen, Y., Han, Y., Cucurull, L., Reynolds, R.W., Rutledge, G. and Goldberg, M. (2010) The NCEP climate forecast system reanalysis. *Bulletin of the American Meteorological Society*, 91, 1015–1057.
- Sapiano, M.R.P. and Arkin, P.A. (2009) An intercomparison and validation of high-resolution satellite precipitation estimates with 3-hourly gauge data. *Journal of Hydrometeorology*, 10, 149–166.
- Schneider, U., Becker, A., Finger, P., Meyer-Christoffer, A., Ziese, M. (2018): GPCC Full Data Monthly Product Version 2018 at 0.25°: Monthly Land-Surface Precipitation from Rain-Gauges built on GTS-based and Historical Data. doi: https://doi.org/10.5676/DWD_GPCC/FD_M_V2018_025
- Schneider, U., Becker, A., Finger, P., Meyer-Christoffer, A., Ziese, M. and Rudolf, B. (2014) GPCC's new land surface precipitation climatology based on quality-controlled in situ data and its role in quantifying the global water cycle. *Theoretical and Applied Climatology*, 115, 15–40. <https://doi.org/10.1007/s00704-013-0860-x>.
- Sevruk, B. and Hamon, W.R. (1984) *International Comparison of National Precipitation Gauges with a Reference Pit Gauge, Instruments and Observing Methods (Report No. 17)*. Geneva: World Meteorological Organization, p. 135.
- Stickler, A., Brönnimann, S., Valente, M.A., Bethke, J., Sterin, A., Jourdain, S., Roucaute, E., Vasquez, M.V., Reyes, D.A., Allan, R. and Dee, D. (2014) ERA-CLIM: Historical Surface and Upper-Air Data for Future Reanalysis. *Bulletin of the American Meteorological Society*, 95(9), 1419–1430. <https://doi.org/10.1175/BAMS-D-13-00147.1>.
- Sun, Q., Miao, C., Duan, Q., Ashouri, H., Sorooshian, S. and Hsu, K.-L. (2018) A review of global precipitation data sets: data sources, estimation, and intercomparisons. *Reviews of Geophysics*, 56, 79–107 <https://doi.org/10.1002/2017RG000574>.
- SUPARCO and FAO (2010) Pakistan Floods/Rains 2010: Rapid Crop Damage Assessment, Series No. 1, Available at http://www.suparco.gov.pk/downloadables/PAKISTAN_FLOODRAIN.pdf
- Syed, F.S., Giorgi, F., Pal, J.S. and King, M.P. (2006) Effect of remote forcings on the winter precipitation of central South-west Asia part 1: observations. *Theoretical and Applied*

- Climatology*, 86(1–4), 147–160. <https://doi.org/10.1007/s00704-0050217-1>.
- Tian, Y.D., Peters-Lidard, C.D., Eylander, J.B., Joyce, R.J., Huffman, G.J., Adler, R.F., Hsu, K.-L., Turk, F.J., Garcia, M. and Zeng, J. (2009) Component analysis of errors in satellite-based precipitation estimates. *Journal of Geophysical Research-Atmospheres*, 114, D24101.
- Treydte, K.S., Schleser, G.H., Helle, G., Frank, D.C., Winiger, M., Haug, G.H. and Esper, J. (2006) The twentieth century was the wettest period in northern Pakistan over the past millennium. *Nature*, 440(7088), 1179–1182. http://www.nature.com/nature/journal/v440/n7088/supinfo/nature04743_S1.html.
- Tuinenburg, O., Hutjes, R.W.A. and Kabat, P. (2012) The fate of evaporated water from the Ganges basin. *Journal of Geophysical Research*, 117, 1–17 <https://doi.org/10.1029/2011JD016221>.
- Turc, L. (1954) Le bilan d'eau des sols: relation entre les précipitations, l'évapotranspiration et l'écoulement. *Annales agronomiques, Série A*, 5, 491–595, 6, 5–131.
- Ullah, W., Wang, G., Ali, G., Hagan, D.F.T., Bhatti, A.S. and Lou, D. (2019) Comparing multiple precipitation products against in-situ observations over different climate regions of Pakistan. *Remote Sensing*, 11, 628. <https://doi.org/10.3390/rs11060628>.
- Ushio, T., Kubota, T., Shige, S., Okamoto, K., Aonashi, K., Inoue, T., Takahashi, N., Iguchi, T., Kachi, M., Oki, R., Morimoto, T. and Kawasaki, Z. (2009) A Kalman filter approach to the global satellite mapping of precipitation (GSMaP) from combined passive microwave and infrared radiometric data. *Journal of the Meteorological Society of Japan*, 87A, 137–151.
- Valéry, A., Andréassian, V. and Perrin, C. (2010) Regionalization of precipitation and air temperature over high-altitude catchments - learning from outliers. *Hydrological Sciences Journal*, 55, 928–940. <https://doi.org/10.1080/02626667.2010.504676>.
- Vila, D., Ferraro, R. and Semunegus, H. (2010) Improved global rainfall retrieval using the special sensor microwave imager (SSM/I). *Journal of Applied Meteorology and Climatology*, 49, 1032–1043.
- Wang, B. and Lin, H. (2002) Rainy season of the Asian-Pacific summer monsoon. *Journal of Climate*, 15, 386–396.
- Weedon, G.P., Balsamo, G., Bellouin, N., Gomes, S., Best, M.J. and Vidale, P.-L. (2014) The WFDEI meteorological forcing dataset: WATCH forcing data methodology applied to ERAInterim reanalysis data. *Water Resources Research*, 50, 7505–7514. <https://doi.org/10.1002/2014WR015638>.
- Wei, J., Dirmeyer, P.A., Wisser, D., Bosilovich, M.G. and Mocko, D. M. (2013) Where does the irrigation water go? An estimate of the contribution of irrigation to precipitation using MERRA. *Journal of Hydrometeorology*, 14, 275–289. <https://doi.org/10.1175/JHM-D-12-079.1>.
- Willmott, C. J., Robeson, S. M., and Matsuura, K. (2017) Climate and other models may be more accurate than reported, *Eos*, 98, <https://doi.org/10.1029/2017EO074939>.
- WMO. (2010) Fact-Finding and Need-Assessment Mission to Pakistan, Mission Report 4–8 November 2010, <https://www.wmo.int/pages/prog/dra/rap/documents/PakistanMissionReport.pdf>
- Xie, P. and Arkin, P.A. (1997) Global precipitation: a 17-year monthly analysis based on gauge observations, satellite estimates, and numerical model outputs. *Bulletin of the American Meteorological Society*, 78(11), 2539–2558.
- Xie, P., Joyce, R., Wu, S., Yoo, S.-H., Yarosh, Y., Sun, F. and Lin, R. (2017) Reprocessed, bias-corrected CMORPH global high-resolution precipitation estimates from 1998. *Journal of Hydro-meteorology*, 18, 1617–1641.
- Yao, T., Thompson, L., Yang, W., Yu, W., Gao, Y., Guo, X., Yang, X., Duan, K., Zhao, H., Xu, B., Pu, J., Lu, A., Xiang, Y., Kattel, D.B. and Joswiak, D. (2012) Different glacier status with atmospheric circulations in Tibetan plateau and surroundings. *Nature Climate Change*, 2(9), 663–667. <https://doi.org/10.1038/nclimate1580>.
- Yatagai, A., Kamiguchi, K., Arakawa, O., Hamada, A., Yasutomi, N. and Kitoh, A. (2012) APHRODITE: constructing a long-term daily gridded precipitation dataset for Asia based on a dense network of rain gauges. *Bulletin of the American Meteorological Society*, 93(9), 1401–1415. <https://doi.org/10.1175/BAMS-D-11-00122.1>.
- Yatagai, A., N. Yasutomi, Maeda, M., Masuda, M., Khadgarai, S. (2018) Impact of nomixed end-of-the-day and station value conservation to represent extremes precipitation over East Asia, (manuscript under preparation http://aphrodite.st.hirosaki-u.ac.jp/product_readme/V1801R1_readme.pdf).
- Yin, S., Xie, Y., Liu, B. and Nearing, M.A. (2015) Rainfall erosivity estimation based on rainfall data collected over a range of temporal resolutions. *Hydrology and Earth System Sciences*, 19, 4113–4126. <https://doi.org/10.5194/hess-19-4113-2015>.
- Zaidi, T.H. (2014) The 2010 Pakistan Floods: Environmental and Economic Impact, Pakistan Studies Programme, Academy of International Studies, Jamia Millia Islamia, New Delhi.

SUPPORTING INFORMATION

Additional supporting information may be found online in the Supporting Information section at the end of this article.

How to cite this article: Dahri ZH, Ludwig F, Moors E, *et al.* Spatio-temporal evaluation of gridded precipitation products for the high-altitude Indus basin. *Int J Climatol*. 2021;1–24. <https://doi.org/10.1002/joc.7073>